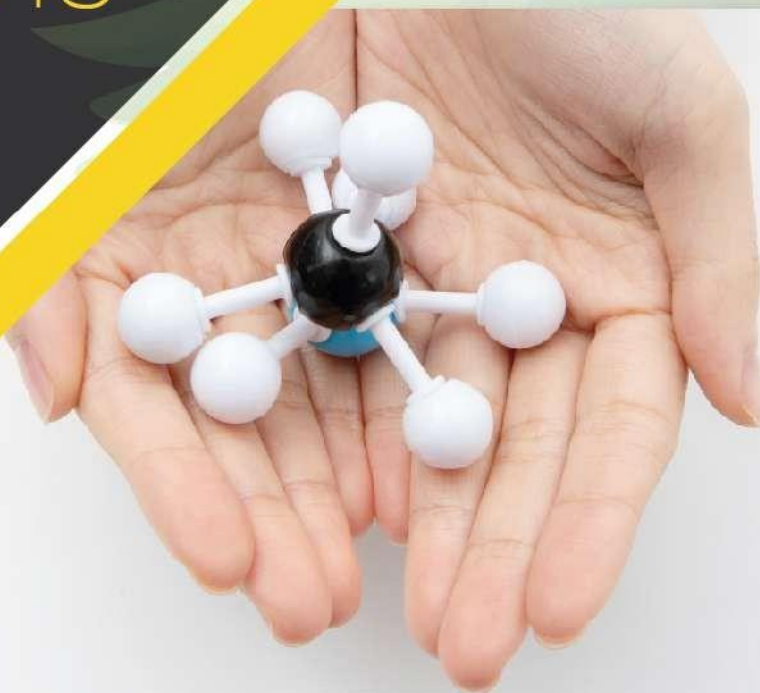




ISSN: 2800-1729

**Edition : Vol 2. Num 2 (2023)**

# Biopolymer Applications Journal



Editor in chief:

**Pr. HAMMICHE Dalila**



UNIVERSITÉ ABDERRAHMANE MIRA - BEJAIA  
FACULTÉ DE TECHNOLOGIE

## **Table of content**

*Chadia IHAMOUCHEEN, Nadia AOUDIA, Hocine DJIDJELLI, Amar BOUKERROU*  
Biodegradation in compost environment of PLA bioplastic containing brown algae biomass.  
Vol 2, N° 2, 2023, pp. 01-08

*Nadira BELLILI, Badrina DAIRI, Nour Elhouda GUIZ, Hocine DJIDJELLI, Amar BOUKERROU*  
Study of the biodegradation of composite materials reinforced with natural resources recovered from industrial areas.  
Vol 2, N° 2, 2023, pp. 09-15

*Badrina DAIRI, Nadira BELLILI, Hocine DJIDJELLI, Amar BOUKERROU*  
Preparation and characterization of Polypropylene Polyethylenterephthalate/wood Fibers composites in the presence of compatibilizer.  
Vol 2, N° 2, 2023, pp. 16-22

*Samira SAHI, Hocine DJIDJELLI, Amar BOUKERROU*  
Evaluation of natural biodegradation of low-density polyethylene/modified corn flour composites.  
Vol 2, N° 2, 2023, pp. 23-27

*Noura HAMOUR, Nadira BELLILI, Badrina DAIRI, Amar BOUKERROU, Johnny BEAUGRAND.*  
Study of PHBV/PP mixtures Preparation and physicochemical characterization.  
Vol 2, N° 2, 2023, pp. 28-34

*Aicha DEHANE, Dalila HAMMICHE, Amar BOUKERROU, Balbir Singh KAITH*  
The effect of a dispersing agent on the properties of polypropylene composites with seaweed fillers.  
Vol 2, N° 2, 2023, pp. 35-40

# Biodegradation in compost environment of PLA bioplastic containing brown algae biomass

Chadia IHAMOUCHEN<sup>1\*</sup>; Nadia AOUDIA<sup>1</sup>; Hocine DJIDJELLI<sup>1</sup>; Amar BOUKERROU<sup>1</sup>

*1: Department of Processes Engineering, Laboratory of Advanced Polymer Materials, University of Bejaia, 06000 Bejaia, Algeria*

\*Corresponding author email: [Chadia.benmerad@univ-bejaia.dz](mailto:Chadia.benmerad@univ-bejaia.dz)

Received 2 May, 2023 ; Accepted : 27 July 2023; Published: 29 July 2023

## Abstract

*This work was focused to the study of the biodegradation of poly lactic acid (PLA) alga composites in compost environment over a period of 50 days. To highlight the interaction between the natural reinforcement and the matrix, an in-situ grafting of maleic anhydride directly during the implementation in the extruder, will be consider to act as a compatibilizing agent (PLA-g-MAH) in the PLA/Algae system. The monitoring of the degradation process was evaluated by infrared structural analysis, mass loss and mechanical tensile analysis. The results revealed that the mass change is positive, suggesting that the chain scission phenomenon predominates over the cross-linking phenomenon. The mass loss increases with the loading rate, processing and composting time. The tensile test study revealed a decrease in stress and elongation and an increase in stiffness with the addition of the untreated filler. The treatment resulted in an improvement in mechanical properties. After 50 days in the compost medium, it was found that all the parameters underwent a clear decrease due to the chain scission reactions by enzymatic hydrolysis. For the FTIR results, an increase in the intensity of the O-H absorption band at 3325 cm<sup>-1</sup> was observed with the untreated load, due to its high OH concentration. With treatment, this decreases, attributed mainly to the decrease in the hydrophilic character of the feed after treatment. After 50 days of composting, we have a decrease of the absorption band located at 1120 cm<sup>-1</sup> (ν C-O) which corresponds to the hydrolysis of the ester bond. The appearance at 1620 cm<sup>-1</sup> of a new band corresponds to the ends of carboxylic acid chains (COO) generated by enzymatic hydrolysis, due to microorganisms that consume lactic acid and surface oligomers*

**Keywords:** Biodegradation, Marine algae, Mechanical property, Poly lactic acid,

## I. Introduction

Nowadays, plastics are present in the life of each individual; they are use in several applications that it would be very difficult to do without them. Nevertheless, beyond their numerous advantages, they generate voluminous waste, which poses enormous problems related to their treatment at the end of life [1]. For this reason, the development of new concepts called "ecological" or "sustainable" materials from renewable sources have emerged. This category of materials can solve the problems of plastic waste, including their ability to degrade naturally in the environment under the action of living organisms and their low rates of emission of greenhouse gases, and they offer distinct advantages over conventional plastics. These new "green" materials generally have the advantage of degrading in a non-toxic way under environmental conditions, without wasting fossil fuels [2]. This phenomenon known as "biodegradation" consists in the degradation resulting from a biological activity (presence of microorganisms) leading to a

modification of the chemical structure of a material. Generally, this process ends with a phase of bio assimilation, which consists in a mineralization of the intermediates of degradation by the microorganisms and ends in aerobic conditions with the production of simple compounds such as carbon dioxide and water as well as a new biomass [3].

Poly lactic acid (PLA) is one of these bioplastics, from the family of aliphatic polyesters. It is considered among the first renewable polymers capable of competing with conventional polymers in terms of performance and environment, because it is three times less CO<sub>2</sub> emitting and already available on the market [4]. Developed in 1960 and 1970 for biomedical applications because of its high price and its ability to be degrade in physiological conditions. However, with the technological revolutions, the tonnages of its production, which explode, and the prices, which fall, the PLA with integrated several other fields of application than the biomedical such as the automobile transport, the packing, the products of hygiene, the electronic material, etc. PLA comes

from renewable resources such as corn or sugar cane. It is obtained by fermentation of sugar or starch, and then transformed into a monomer: the lactide. The polymerization of the latter makes it possible to obtain PLA [5, 6]. To improve the different properties of this biopolymer, it is mixed with synthetic polymers or by incorporating natural reinforcement, which allows the development of bio composites. In this study, the choice of the reinforcement was made on the brown algae. Algae are living chlorophyllous photosynthetic organisms found in aquatic environments [7]. They vary greatly in shape, colour and size. Some are microscopic, others macroscopic. Their processing has developed massively in recent years, with 25 million tons harvested each year for a market estimated at more than \$6 billion. They are an important source of polysaccharides (carrageenans, alginates, agar...) whose physicochemical, stabilizing and gelling properties are of interest to many industrial sectors [8].

The reinforcement of composite materials by plant fillers is in full expansion of academic and industrial research. Their potential in terms of mechanical and environmental gains is undeniable, even if their sensitivity to humidity remains a barrier [9, 10]. The innovation in this type of material concerns the interaction between these natural fibers and the matrix, which leads to incompatibility problems. For this reason, physical or chemical modifications of the filler are most often used. This work has a double objective; the first is to develop a new material based on a biodegradable PLA matrix and brown algae. To highlight the interaction between the natural reinforcement and the matrix, an in-situ grafting of maleic anhydride directly during the implementation in the extruder, to obtain PLA-g-MA, which will be considered to act as a compatibilizing agent in the PLA/Algae system. The second is the monitoring of physico-chemical properties for a better understanding of the mechanisms involved in the degradation process.

## II. Material and methods

### II.1. Materials

#### II.1.1. Poly (lactic acid) (PLA)

The matrix used is the Poly (lactic acid) (PLA) produced by Nature Works LLC (United States), is supplied by the company Nature Plast (France), under the trade name Ingeo "7001D", in the form of granules (figure III.1), specially designed for injection blow molding machines. Its main characteristics are grouped in table 1.

**Table 1:** Characteristics of the PLA matrix.

Properties	Unit
Appearance	Transparent
Melt index (210 °C, 2.16 Kg)	6 g/10 min

Melting temperature	145-160 °C
Glass transition temperature	55-60 °C
Density	1.24
Number average molar mass	75 000 g.mol <sup>-1</sup>

#### II.1.2. Brown seaweed meal

The load used in this study is the flour of brown algae of the species *Fucus serratus* collected on the beach of Fort-bloqué in Ploemeur, Lorient (France) during January. Scientific name *Fucus serratus*, of color brown olive with the blackish green. This rockweed presents a very flat thallus has divided fronds, with toothed edges, measures in general between 40 and 80 cm length (figure 1).



**Figure 1:** The species *Fucus serratus* (brown alga)

Before their use, these algae have undergone several pre-treatments, namely: Sorting: Manually in order to eliminate any source of contamination. Washing: The algae are rinsed twice with tap water and then twice with distilled water to remove all kinds of contamination: sand, insects, water-soluble compounds. Drying: The seaweeds underwent a preliminary drying in the open air for three days and then in an oven at 80 °C for 24 hours to evaporate the water. Grinding and sieving: The algae were ground in a laboratory grinder and sieved through a 250µm sieve. Then preserved in hermetically sealed plastic bags.

**II.1.3. Other products:** Maleic Anhydride (MAH) 99%, and Dicumyl peroxide (DCP) 98% were purchased from Sigma-Aldrich, are used for in situ grafting directly in a brabender on the PLA chain to obtain PLA-g-MAH, which will be considered as a compatibilizing agent in the PLA/alga system. All of PLA and algae powder were dried under vacuum oven at 60°C overnight before use.

#### II.1.4. Compost

The compost used in the study was recovered from a local company in the region of El-Kseur, Bejaia, Algeria. The main

characteristics of this compost are visualized below in figure 2.



Figure 2: The main characteristics of the compost used

## II.2 Methods of elaboration of PLA/algae biocomposites

### II.2.1. Formulations

The biopolymer (PLA) and the filler (alga powder) are previously dried at 80° C in an oven for 24 hours, in order to eliminate the water content. The different percentages were weighed, and then mixed manually. In total, seven formulations were prepared, according to the proportions indicated in Table 2.

Table 2: Compositions of the different formulations

Formulations	Noted	PLA	Algae powder	Maleic anhydride (MAH)	Benzoyl peroxide (BOP)
PLA	F0	100	0	0	0
PLA/10% Algae	F10	90	10	0	0
PLA/20% Algae	F20	80	20	0	0
PLA/30% Algae	F30	70	30	0	0
PLA /10% Algae /PLA-g-MAH	F10g	85	10	3	1,5
PLA /20% Algae /PLA-g-MAH	F20g	75	20	3	1,5
PLA /30% Algae /PLA-g-MAH	F30g	65	30	3	1,5

### II.2.2. Compression molding

The PLA, PLA/algae formulations with and without compatibilizer are prepared in the molten state in a brabender of model W50 EHT at 185 °C with a rotation speed of 50 rpm for a residence time of 8 min. The mixture is recovered for use in compression molding under the following working conditions: Temperature of 170 °C, under a pressure of 80 KN and during a residence time of 5 min (a preheating of 3 minutes is carried out until a preliminary fusion of the mixture, in order to avoid the presence of air bubbles). Plates of 1 mm thickness are obtained, and then are cut to be used in the various tests.

### II.2.3. Biodegradation test

The biodegradability tests were performed in polyethylene bins at room temperature in the composting environment. Rectangular (length 70 mm, width 10 mm, thickness about 1 mm) and square (20 x 20 mm) samples are buried in containers containing 2 to 3 kg of industrial compost. A sample is taken every 25 days over a period of 50 days, with weekly watering with borehole water [11].

### II.2.4. Mass variation

The observation of mass variation is simple and effective method. It does not require special instrumentation, and is widely used for the determination of the biodegradability of polymers in the solid state. Samples are weighed before burial in the compost to record the initial mass ( $m_0$ ). After collection, the samples are wiped, dried in an oven at 60 °C for 2h, and then weighed to obtain the average mass ( $m_t$ ). The mass loss is calculated by the equation (1) :

$$\Delta m \% = \frac{m_0 - m_t}{m_0} \cdot 100 \dots\dots\dots (1)$$

With:  $\Delta m$ : Variation in mass

$m_t$ : Mass of the sample after burial.

$m_0$ : Initial mass of the sample before burial

### II.2.5. Fourier Transform infrared analysis

Spectroscopy in general is a method of analysis based on the study of interactions between matter and electromagnetic radiation. The Fourier Transform Infrared (FTIR) is a very effective method for identifying organic and inorganic molecules from their vibrational properties (deformation, elongation). It allows studying the structural modifications of polymers resulting from chemical treatments, degradation or aging of various origins.

The FTIR spectra of the different samples were recorded in absorbance mode using a SHIMADZU FTIR-8400 S model infrared spectrophotometer, with a resolution of 4 cm<sup>-1</sup> in the range 400-4000 cm<sup>-1</sup> with a number of scans of 32. The analysis is performed on PLA/Algae composite films.

### II.2.6 Tensile test

The tensile test consists in determining the deformation of the specimen under the application of a load with a defined speed. This test makes it possible to determine the modulus of elasticity E (MPa) or Young's modulus, the stress at break ( $\sigma$ ) and the elongation at break ( $\epsilon$ ). The tensile test was conducted at the research unit of the University of Boumerdes at room temperature on a traction machine brand "Zwick type 8306" controlled by software. The speed of traction was kept constant at 5 mm /min. On average, three tests were carried out for each formulation.

### III. Results and discussion

#### III.1 Mass loss

The figure 3 shows the variation in mass of the PLA/algae composites as a function of the composting time. It can be seen that the variation is positive (loss of mass), which suggests that the phenomenon of chain scission predominates over the phenomenon of cross-linking [12]. We can also note that the longer the biodegradation time, the greater the loss of mass is for all the formulations developed.

✓ The results obtained reveal that PLA reaches a lower degree of disintegration, with mass losses of 0.25% and 4% after 25 and 50 days. This low biodegradation reveals the difficulty that microorganisms find to attack this material.

✓ On the other hand, the composites loaded with the untreated seaweed powder, they present a higher biodegradation compared to the virgin PLA, due in particular to their natural origin that contributes to their biodegradation more easily. This increase increases with the loading rate and the composting time. As an example, at 25 days, 4, 11 and 16% were recorded, for the formulations F10, F20 and F30 respectively and after 50 days, the loss of mass reached 11, 14 and 23% for the same formulations.

✓ With the treatment, the mass loss decreases compared to the untreated composites, this is probably due to the presence of the PLA-g-MAH compatibilizing agent, since the latter contains several hydrophilic sequences on the main chain that can be easily accessible sites by microorganisms or their secretion products.

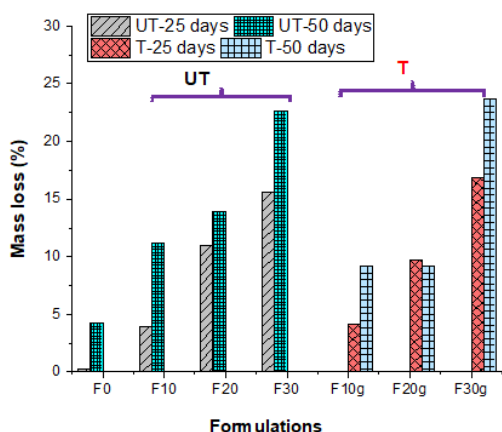


Figure 3: Evolution of mass loss of treated and untreated composites before and after 50 days in compost.

#### III.2 Fourier transform infrared analysis (FTIR)

##### III.2.1. Effect of the load

The figure 4 shows the FTIR spectrum of virgin PLA.

The spectrum of PLA reveals the presence of several absorption bands [13, 14]:

- Two peaks centred at 3503 and 2970  $\text{cm}^{-1}$  correspond to the region of the hydroperoxide groups, attributed to the elongation vibrations of the -CH groups.
- A broad and intense band centred at 1734  $\text{cm}^{-1}$ , corresponding to the absorption of the C=O carbonyl groups of the esters present in PLA.
- A series of broad absorption bands centred at 1300 and 1465  $\text{cm}^{-1}$ , attributed to the -CH<sub>3</sub> groups present in the form of a mixture of vibrations, symmetrical and asymmetrical deformations.
- A series of bands at 1118 and 1020  $\text{cm}^{-1}$  corresponding to the elongation vibrations of C-O groups.
- A peak at 866  $\text{cm}^{-1}$  is attributed to the elongation vibrations of C-C
- we could also note on the spectrum, that there was a rather spread out peak, centered at 3500  $\text{cm}^{-1}$  which is typical of the presence of hydroxyl groups -OH, in our case they are the ends of chains.

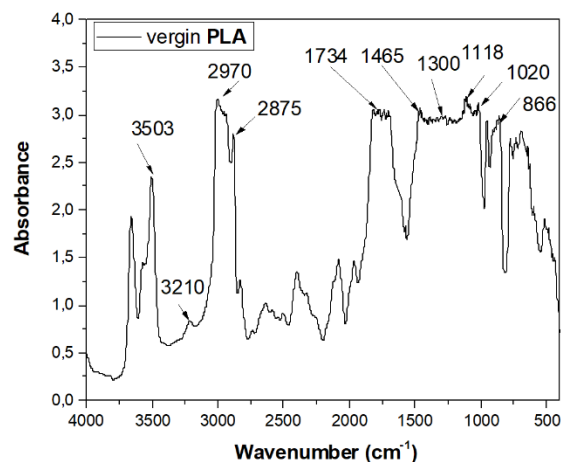


Figure 4: FTIR spectrum of virgin PLA.

The FTIR spectra of the PLA/algae composites are shown in Figure 5. The same peaks appear as for PLA, but with different intensities. As an example, an increase in intensity is recorded for the absorption band recorded at 3325  $\text{cm}^{-1}$  that corresponds to the stretching vibration of the OH bond of the absorbed water, which reflects the hydrophilic character of the charge. Moreover, in the peaks at 1620  $\text{cm}^{-1}$ , which correspond to the carboxylic groups COO, whose contribution comes from the alginates contained in the brown algae [15].

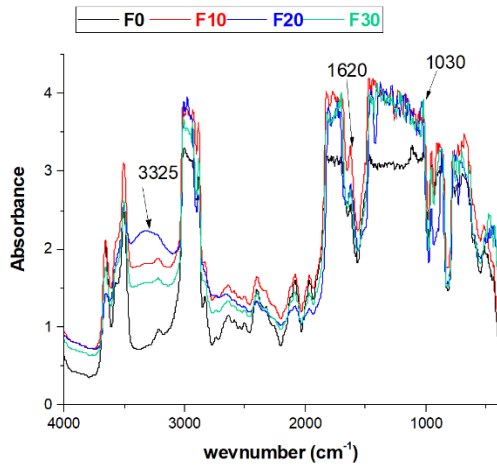


Figure 5: FTIR spectrum of PLA/algae composites

### III.2.2. Treatment effect

The compatibilizing agent PLA-g-MAH, was used to improve the interfacial adhesion between the filler and the matrix, by creating bonds that did not exist until then and lowering the hydrophilic character of the natural filler used, and to highlight this treatment, the FTIR spectra of the composites untreated and treated with PLA-g-MAH are shown in Figure 6.

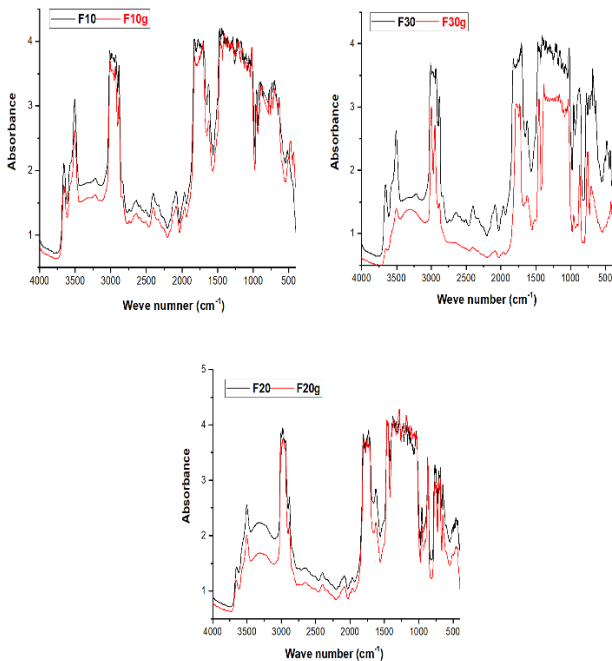


Figure 6: FTIR spectra of untreated and treated composites

Effectively, we notice that the treated composites F10g, F230g and F30g show an absorption band that is located in the region 3500 and 3000  $\text{cm}^{-1}$ , and which corresponds to the elongation

vibrations of the hydroxyl groups (-OH), for which we register a decrease in its intensity compared to the untreated composites. This decrease is mainly attributed to the decrease of the hydrophilic character of the filler after the treatment with PLA-g-MAH.

### III.2.3. Aging effect

The pristine PLA samples, recovered after 50 days in compost media, were analysed by FTIR and the results are shown in Figure 7. The superposition of the PLA spectra at 0 day and 50 days highlights the decrease of an absorption band at 1120  $\text{cm}^{-1}$  and the appearance of a new band at 1620  $\text{cm}^{-1}$ .

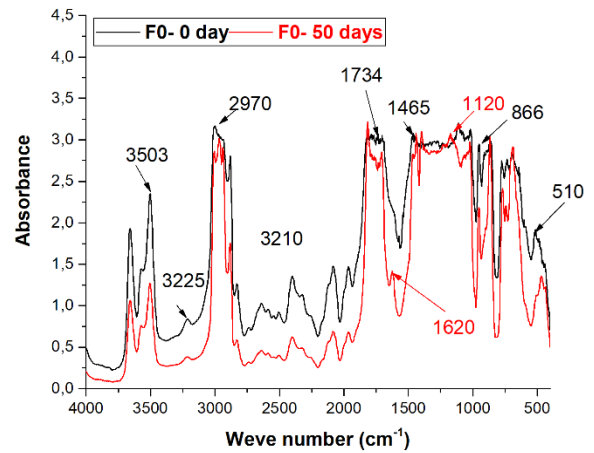


Figure 7: FTIR spectrum of PLA before and after 50 days in compost

According to the literature [16], the decrease of the absorption band located at 1120  $\text{cm}^{-1}$  (vibration of the CO groups) would correspond to the hydrolysis of the ester bond. The appearance of a new absorption band at 1620  $\text{cm}^{-1}$  corresponds to the ends of carboxylic acid chains generated by enzymatic hydrolysis. The formation of carboxylate ions at the ends of the chains would be due to the microorganisms consuming the lactic acid and the surface oligomers.

During the degradation process, the concentration of  $\text{COO}^-$  is increased by the presence of carboxyl groups resulting from the hydrolysis mechanism of the ester functions. With each hydrolyzed ester bond, a new carboxylic acid chain end is formed, and this catalyzes the hydrolysis reaction of the remaining ester bonds. The concentration of the concentration of carboxyl groups increases as the process proceeds, accelerating the degradation.

The spectra of the PLA/algae composites are shown in Figure.8.

The same observation is made for the treated and untreated PLA/algae composites, The spectra highlight the decrease of the absorption band at 1120  $\text{cm}^{-1}$ . The decrease of the

absorption band located at  $1120\text{ cm}^{-1}$  (vibration of the CO groups) would correspond to the hydrolysis of the ester bond.

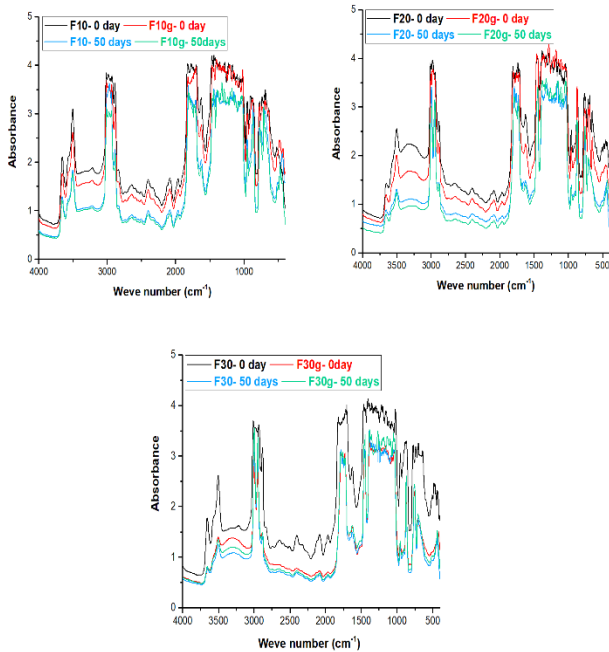


Figure 8: FTIR spectra of treated and untreated composites before and after 50 days in compost

### III.3 Tensile test

#### III.3.1. Tensile strength

The evolution of the stress at break of the PLA/algae composites after 50 days in compost medium was represented in figure 9.

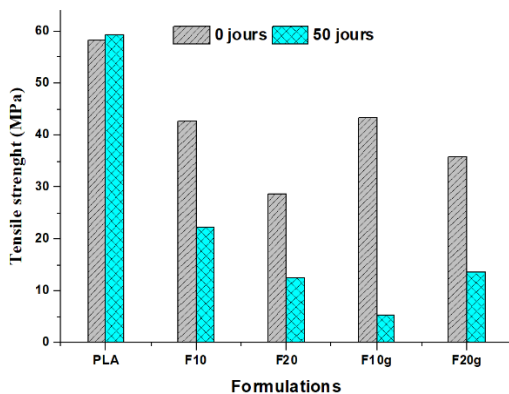


Figure 9: Evolution of the stress at break of PLA/Alga composites before and after composting

- It can be seen that the tensile strength of the composites decreases with the introduction of the algal filler and this decrease was accentuated with the increase of the filler rate; it reaches almost half the value of PLA for 30 % wt. of filler going from 58.8 MPa to 30 MPa. This decrease is

mainly attributed to the poor dispersion of the filler, forming agglomerates, which induces a decrease in the bonding strength between the matrix and the filler and consequently the failure of the stress propagation [17, 18].

- The addition of 5% PLA-g-MAH slightly improved the strength values of the formulations, indicating better stress transfer from the matrix to the filler in the presence of the compatibilizer.
- After 50 days in the compost medium, it can be seen that the stress at break for the PLA matrix was not influenced too much, increasing from 58 to 59 MPa. On the other hand, a clear decrease of the stress is recorded for the untreated and treated composites. It should be noted that the F30 and F30g formulations were not tested, as the specimens were found broken in the composting bins, during sampling after 50 days.

#### III.3.2. Elongation at break

The evolution of elongation at break of untreated and treated composites as a function of composting time is shown in Figure 10.

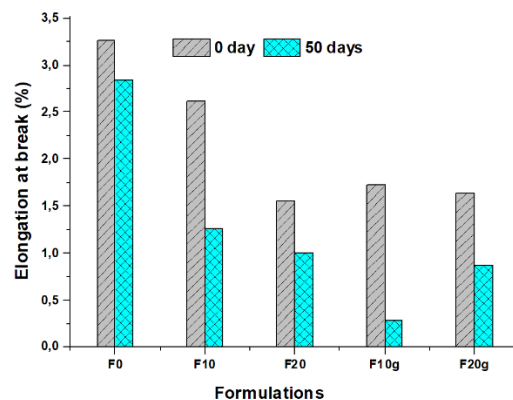


Figure 10: Evolution of elongation at break of PLA/Algae composites before and after composting

- The elongation at break of the composites decreases with the increase of the algae powder content, reaching a minimum value (1%) at 30% by weight of filler. This decrease is attributed to the increased stiffness provided by the filler, which reduces the plasticity range of the matrix and thus limits its deformation and flow, which is a common characteristic of reinforced thermoplastic composites.
- The addition of PLA-g-MAH further reduces the elongation at break for the 10% filled composites, but slightly increases for the 20% filled composites. This increase is due to the accounting agent acting as a plasticizer.
- After 50 days in the compost, we notice that the trend of all the formulations is characterized by a significant decrease in the elongation at break. The decrease in elongation at break of PLA and F10 and F20 composites was estimated at 12.89;

51.73 and 35% respectively. The same finding for the F10g and F20g formulations estimated at 83.73 and 46.62%. This sudden decrease in deformation with the time of composting is due to the reactions of scission of the chains, increasing the density of molecules links between the crystalline phases, and consequently decrease in deformation [19].

### III.3.3. Young's modulus

The histograms in figure 11 show the evolution of the Young's modulus of the different samples as a function of the composting time.

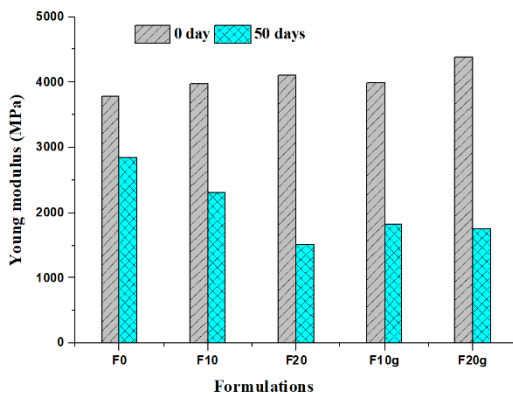


**Figure 11:** Evolution of the Young's modulus of PLA/Alga composites before and after composting

- The addition of the algae powder results in an increase in Young's modulus, suggesting a microstructural change within the polymer. With a 26% improvement with the addition of 30% algae powder, which is due to the increase in the rigid nature of the filler [20, 21]
- Young's modulus values are higher for composites compatibilized with PLA-g-MA than non-compatibilized composites; this can be explained by the correlation between the improvement of interfacial adhesion between matrix and filler in the presence of compatibilizer, and the increase in tensile modulus.
- The modulus decreases as a function of composting time regardless of the composition of the sample. This decrease is due to the phenomenon of chain splitting, where the cut chain fragments have more freedom and more movement [22; 23].

## IV. Conclusions

This work, relates to the study of the biodegradation of biocomposites poly (lactic acid) reinforced by the powder of brown alga (PLA/Alga) in a compost medium over a period of 6 months, but because of lack of time, we carried out just two samples after 25 and 50 days and the study is still in progress. At the end of this study, the results obtained allowed us to draw the following conclusions:

The mass variation is positive, which suggests that the chain scission phenomenon predominates over the cross-linking phenomenon. The loss of mass increases with the loading rate, the treatment and the composting time.

The tensile test study revealed a decrease in stress and elongation and an increase in stiffness with the addition of the untreated filler. The treatment resulted in an improvement in mechanical properties. After 50 days in the compost medium, it was found that all the parameters underwent a clear decrease due to chain scission reactions by enzymatic hydrolysis. For the FTIR results, an increase in the intensity of the O-H absorption band at  $3325\text{ cm}^{-1}$  was observed with the untreated load, due to its high OH concentration. With treatment, the latter decreases, attributed mainly to the decrease in the hydrophilic character of the feedstock after treatment. After 50 days of composting, we have a decrease of the absorption band located at  $1120\text{ cm}^{-1}$  ( $\nu$  C-O) which corresponds to the hydrolysis of the ester bond. The appearance at  $1620\text{ cm}^{-1}$  of a new band which corresponds to the ends of carboxylic acid chains (COO) generated by an enzymatic hydrolysis, due to microorganisms which consume lactic acid and surface oligomers. Following the spectral analysis carried out by FTIR, the spectrum showed that the introduction of the agent Maleic Anhydride (MAH) in the PLA/Alga composites reduces in a remarkable way the hydroxyl groups, since the latter contains several hydrophilic sequences on the main chain that can be sites easily accessible by the microorganisms or by their secretion products.

The main conclusions of the study may be presented in a short Conclusions section, which may stand alone or form a subsection of a Discussion or Results and Discussion section.

## References

- [1] Emma M.N. Polman, Gert-Jan M. Gruter, John R. Parsons, Albert Tietema. Comparison of the aerobic biodegradation of biopolymers and the corresponding bioplastics: A review. *Science of the Total Environment* 753, 141953, 2021. <https://doi.org/10.1016/j.scitotenv.2020.141953>
- [2] J.-G. Rosenboom, R. Langer, G. Traverso, Bioplastics for a circular economy, *Nat. Rev. Mater.* 7 117–137, 2022. <https://doi.org/10.1038/s41578-021-00407-8>
- [3] S. K. Awasthi, M. Kumar, V. Kumar, S. Sarsaiya, P.Anerao, P. Ghosh, L.Singh, H. Liu, Z. Zhang, M. Kumar Awasthi. A comprehensive review on recent advancements in biodegradation and sustainable management of biopolymers. *Environmental Pollution* 307, 119600, 2022. <https://doi.org/10.1016/j.envpol.2022.119600>

- [4] A. Le Duigou, A. Bourmaud, C. Baley, In-situ evaluation of flax fibre degradation during water ageing. *Industrial Crops and Products*, 70, 204-210, 2015. <https://doi.org/10.1016/j.indcrop.2015.03.049>
- [5]: D. Garlotta, A literature review of poly (lactic acid). *Journal of Polymers and the Environment*, 9(2), 63-84, 2001. <https://doi.org/10.1023/A:1020200822435>
- [6] A. Karimah, M. R. Ridho, S. S. Munawar, D. Sudarwoko Adi, Ismadi, R. Damayanti, B. Subiyanto, W. Fatriasari, A. Fudholi. A review on natural fibers for development of eco-friendly bio-composite: characteristics, and utilizations. *Journal of materials research and technology*; 13: 2442 -2458, 2021. <https://doi.org/10.1016/j.jmrt.2021.06.014>
- [7] Ullah K, Ahmad M, Sofia Sharma VK, Lu P, Harvey A, Zafar M, et al. Assessing the potential of algal biomass opportunities for bioenergy industry: a review. *Fuel*; 143, 414–23, 2015. <https://doi.org/10.1016/j.fuel.2014.10.064>
- [8] H.P.S. Abdul Khalil, C.K. Saurabh, Y.Y. Tye, T.K. Lai, A.M. EasaaE Rosamah, M.R.N. Fazita, M.I. Syakir, A.S. Adnan, H.M. Fizree, N.A.S. Aprilia, A. Banerjee. Seaweed based sustainable films and composites for food and pharmaceutical applications: A review. *Renew. Sust. Energy Rev.* 77 353–362, 2017. <https://doi.org/10.1016/j.rser.2017.04.025>
- [9] L. Kerni, S. Singh, A. Patnaik, N. Kumar, A review on natural fiber reinforced composites, *Mater. Today Proc.* 28 1616–1621, 2020. <https://doi.org/10.1016/j.matpr.2020.04.851>
- [10] M. Gupta, R. Srivastava, Mechanical properties of hybrid fibers-reinforced polymer composite: a review, *Polym.-Plast. Technol. Eng.* 55 (6) 626–642, 2016. <https://doi.org/10.1080/03602559.2015.1098694>
- [11] Shi, H., Wang, X.C., Li, Q., Jiang, S., Degradation of typical antibiotics during human feces aerobic composting under different temperatures. *Environ. Sci. Pollut. Res. Int.* 23 (15), 15076–15087, 2016. <https://doi.org/10.1007/s11356-016-6664-7>
- [12] R. Kumar, M. K. Yakubu, R. D. Anandjiwala. Biodegradation of flax fiber reinforced poly lactic acid. *eXPRESS Polymer Letters* Vol.4, No.7 423–430, 2010. <https://doi.org/10.3144/expresspolymlett.2010.53>
- [13] T.Gerard, T Budtova.. Morphology and molten-state rheology of polylactide and polyhydroxyalkanoate blends. *European polymer journal*, 48(6), 1110-1117, 2012. <https://doi.org/10.1016/j.eurpolymj.2012.03.015>
- [14] A.Rapacz-Kmita, E. Stodolak-Zych, M. Dudek, B. Szaraniec, A. Rozycka, M. Mosialek, L. Mandecka-Kamien., Degradation of nanoclay-filled polylactide composites. *Physicochemical Problems of Mineral Processing*, 49(1), 91-99, 2013. <http://dx.doi.org/10.5277/ppmp130109>
- [15] J. Jayaraj, A. Wan, M. Rahman, Z. K. Punja, Seaweed extract reduces foliar fungal diseases on carrot. *Crop Protection*, 27(10), 1360-1366, 2008. <https://doi.org/10.1016/j.cropro.2008.05.005>
- [16] H. P. Zhang, J. M. Ruan, Z. C. Zhou, Y. J. Li. Preparation of monomer of degradable biomaterial poly (L-lactide). *Journal of Central South University of Technology*, 12(3), 246-250, 2005. <https://doi.org/10.1007/s11771-005-0136-4>
- [17] C. Hellio, D. De La Broise, L. Dufosse, Y. Le Gal, N. Bourgougnon, Inhibition of marine bacteria by extracts of macroalgae: potential use for environmentally friendly antifouling paints. *Marine environmental research*, 52(3), 231-247, 2001. [https://doi.org/10.1016/S0141-1136\(01\)00092-7](https://doi.org/10.1016/S0141-1136(01)00092-7)
- [18]: Y. H. Kim, J. H Kim, H. J. Jin, S. Y. Lee. Antimicrobial activity of ethanol extracts of *Laminaria japonica* against oral microorganisms. *Anaerobe*, 21, 34-38, 2013. <https://doi.org/10.1016/j.anaerobe.2013.03.012>
- [19] Tao Yu, Ning Jiang, Yan Li. Study on short ramie fiber/poly(lactic acid) composites compatibilized by maleic anhydride. *Composites Part A: Applied Science and Manufacturing*. 64, 139-146, 2014. <https://doi.org/10.1016/j.compositesa.2014.05.008>
- [20] T. Budtova, M. Bulota. PLA/algae composites: Morphology and mechanical properties. *Composites: Part A* 73, 109 -115, 2015. <https://doi.org/10.1016/j.compositesa.2015.03.001>
- [21] T. Bulota M, Budtova . Valorisation of macroalgae industrial by-product as filler in thermoplastic polymer composites *Composites Part A: Applied Science and Manufacturing* Vol 90, 271-277, 2016. <https://doi.org/10.1016/j.compositesa.2016.07.010>
- [22] Judith Sarasa, Jose M. Gracia, Carlos Javierre. Study of the bio-disintegration of a bioplastic material waste. *Bioresource Technology* 100 3764–3768, 2009. <https://doi.org/10.1016/j.biortech.2008.11.049>
- [23]: S. K Saha, H. TsujiHydrolytic. Degradation of Amorphous Films of l-Lactide Copolymers with Glycolide and d-Lactide. *Macromolecular materials and engineering*, 291(4), 357-368, 2006. <https://doi.org/10.1002/mame.200500386>

# Study of the biodegradation of composite materials reinforced with natural resources recovered from industrial areas.

Nadira BELLILI<sup>1,2\*</sup>; Badrina DAIRI<sup>1,2</sup>; Nour Elhouda GUIZ<sup>1</sup>; Hocine DJIDJELLI<sup>2</sup>; Amar BOUKERROU<sup>2</sup>

1: Department of Petrochemical and Process Engineering, Faculty of Technology, Skikda University 20 Aout – 1955 – Algeria

2: Department of Process Engineering, Faculty of Technology, Laboratory of Advanced Polymer Materials (LMPA), Abderrahmane MIRA University, Béjaïa 06000, Algeria

\*Corresponding author email: n.bellili@univ-skikda.dz dina\_1961s@yahoo.fr

Received: 5 May 2023; Accepted : 27 July 2023; Published: 29 July 2023

## Abstract

*The aim of our work is to contribute to the search for solutions to the problem linked to environmental pollution by plastic materials and lignocellulosic waste. Composites based on polyvinyl chloride/olive pomace flour (PVC/FGO) with 20% fiber content were prepared. The lack of compatibility between plant fibers and some polymers is due to the hydrophilic nature of plant fibers and the more hydrophobic nature of the matrix. This incompatibility causes poor dispersion of the fibers and the formation of a heterogeneous material whose overall mechanical properties are not satisfactory. In order to improve adhesion at the fiber/matrix interface, the fibers were modified by gamma irradiation. To complete this work, it is essential to carry out an in-depth study of the biodegradation of the materials produced. The PVC/FGO composites were subjected underground under environmental conditions. The changes induced by the exposure of composite materials to biodegradation were evaluated by optical microscopy and the measurement of mass loss.*

**Keywords:** Composites, Natural Resources, Biodegradation

## I. Introduction

Plant-based fiber composites are currently experiencing strong growth due in particular to the growing interest in them from the automotive industry. These fibers present an excellent alternative to glass fibers from an environmental point of view due to their biodegradability and their much more neutral combustibility in terms of the release of harmful gases or solid residues [1]. However, plant fibers, although they have many qualities, have some major flaws when it comes to combining them with polymers [2]. Modification of the surface of the fibers is generally necessary in order to improve their adhesion with a polymeric matrix and to reduce the absorption of humidity. It has been shown that appropriate treatment applied to the fibers can result in compatibility with the polymer matrix, which improves the quality of the composites [3]. PVC/wood composites are widely used in the field of building materials, as they offer acceptable mechanical properties, good chemical and fire resistance, low water absorption and long service life [4]. In this context, the main objective of this thesis is the characterization of a composite material based on PVC reinforced with untreated olive pomace fibers and treated with gamma irradiation in order to improve the mechanical and thermal properties. Subsequently, we conducted an in-depth study of the biodegradation of the materials produced. Several

characterization methods were used such as SEM, TGA, IR, to monitor the changes in the characteristics of this composite and its biodegradation over time.

## II. Material and methods

PVC type 3000H manufactured by CIRES (USA) was used to prepare the formulations. The plasticizer added is dioctylphthalate (DOP). The heat stabilizer used, of industrial quality, is a mixture of calcium and zinc salts (Ca/Zn), and stearic acid as a lubricant. The natural filler used is olive pomace flour, a by-product of oil mills. The pomace was brought from the Tazmalt region (Beni Mellikeche) of the wilaya of Bejaia, Algeria [1].

### A. Pretreatment of olive pomace

The olive pomace were washed with cold water then with hot water to remove the remains of the pulp, followed by drying at room temperature for 48 hours, drying is completed in an oven for 24 hours at 105°C. The grinding was carried out with traditional methods using a manual stone mill then with a coffee grinder. To have a homogeneous particle size, sieving was carried out using a controlab type sieve shaker "Automatic Sieve Shaker D411". The dimension of the flour is less than 100 µm. The olive pomace flour is washed with acetone for 24 hours using a soxhlet to eliminate any contamination or

impurity. The recovered flour is steamed at a temperature of 100°C for 24 hours [1].

### B. Chemical composition of olive pomace

The chemical composition of olive pomace flour was determined at the laboratory of advanced polymer materials, University of Bejaia.

**Table 1** Chemical compositions of olive pomace flour [1].

Composition	rate in % by mass
Cellulose	40,56
Hémicellulose	18,10
Lignin	23,43
MS	92,10
Th	07,90
MM	03,61
MG	14,31

### C. Samples preparation

The PVC resin and the various additives are mixed in a beaker using a spatula until the mixture becomes homogeneous. 1 mm thick sheets of F0 (virgin PVC) and composites loaded with 20% untreated and treated pomace flour with  $\gamma$  radiation, were prepared using a LE SCUYER brand calender type M89. The temperature along the two-roll mixer is maintained at 160°C, for a residence time of 15 min. The sheets are then cut into the appropriate shape for the characterize [1].

### D. Gamma irradiation of samples

The charge was irradiated at the nuclear research center in Algiers (CRNA) using the gamma radiation source. These gamma rays are obtained from the decay of Co60. Several formulations have been prepared, varying the dose of gamma irradiation [1]. An unfilled PVC formulation denoted F0.

A PVC formulation filled with 20% untreated olive pomace rated F20.

A formulation of PVC filled with 20% olive pomace treated with gamma irradiation at doses of 10; 25; 50; 60 and 70KGy rated F20CH10KGy, F20CH25KGy, F20CH50KGy, F20CH60KGy and F20CH70KGy respectively.

Olive pomace flour treated with gamma radiation at doses of 10; 25; 50; 60 and 70KGy, denoted by: F, F10 KGy, F25 KGy, F50 KGy, F60 KGy and F70 KGy respectively.

**Table 2** Mass composition of PVC/ olive pomace formulations [1]

Formulation	F0	F20	F
Products		F20CH10KGy	F10KGy
		F20CH25KGy	F25KGy
		F20CH50KGy	F50KGy
		F20CH60KGy	F60KGy
		F20CH70KGy	F70KGy
PVC	100	80	0
DOP	30	30	0
Ca/Zn	2	2	0
Stearic acid	06	0.6	0

Olive flour	pomace		
	0.3	20	100
PVC	100	80	0

### E. Sample characterization by Scanning Electron Microscopy (SEM)

Scanning electron microscopy was used to characterize the surface condition of the filler. The equipment used is a Philips model scanning electron microscope at the macromolecular materials laboratory (LMM) of INSA Lyon. [1].

### F. Sample characterization by Thermogravimetric Analysis (ATG/DTG)

Thermogravimetric analysis (TGA) is based on the determination of the mass loss that a sample undergoes during its heating. These mass losses are recorded as a function of temperature in an appropriate interval. This method allows us to graphically determine the decomposition temperature of the sample. Measurements of the thermal stability and the rate of decomposition of the various samples are carried out using a SETERAM TGT-DTA type thermogravimetric device controlled by a microcomputer. A mass of 10 to 15 g of a sample is introduced into an aluminum crucible and the loss in mass of the sample as a function of temperature is recorded with a heating rate of 10°C/min in a temperature range ranging from 25°C to 700°C [1].

## III. Study of the biodegradation of prepared composite materials

The PVC/FGO composites that were subjected underground under environmental conditions, were evaluated by optical microscopy, the measurement of mass loss and Fourier transform infrared spectroscopy.

### A. Surface characterization of composites by optical microscopy

The observation by optical microscopy of the untreated and treated samples allows us to visualize the surface condition of different composites under the effect of irradiation and after their exposure to climatic conditions. Observations are made using a euromex optical microscope with 100x magnification.

### B. Mass loss

After immersing the films to be studied underground for an extended period, samples are regularly taken. The operating mode consists in weighing the samples before their immersions in the basement (m0).

In each collection, the samples are removed from the soil and wiped off any surface soil that covers them, using a clean, dry

cloth. Each specimen was weighed again (mass  $m_i$ ). The mass loss  $m$  (%) is calculated by the following equation:

$$m (\%) = ((m_i - m_0) / m_0) \times 100 \quad \text{Eq. (1)}$$

Where:

$m$  (%): The mass loss  $m$  (%)

$m_0$ : The mass, in grams, of the initial specimen and before immersion;

$m_i$ : The mass, in grams, of the specimen after immersion.

#### IV. Results and discussion

##### A. Study of the morphology of olive pomace flour by the scanning electron microscope (SEM)

Fig. 1 shows a scanning electron micrograph (SEM) of untreated Fig. 1.a, and treated olive pomace flour at 70 kGy Fig.1.b. It is observed that the untreated filler tends to agglomerate, furthermore, after the irradiation of the olive pomace flour, the size of the particles are reduced and are well dispersed [1]. A similar result was found by Bhowmick A-K., for clay treated by electron beam irradiation [2].

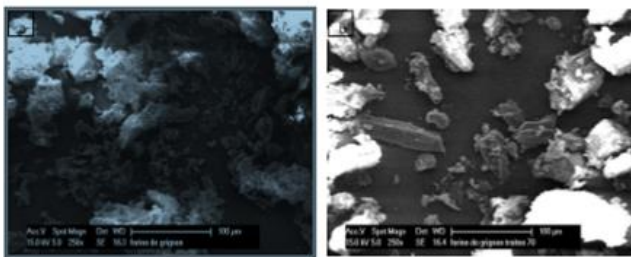


Figure 1. SEM micrograph of olive pomace flour : a) F, b) F70 kGy.

##### B. Effect of gamma irradiation on the thermal stability of olive pomace flour

To study the thermostability of olive pomace flour after treatment by gamma irradiation, we used thermogravimetry which consists in monitoring the evaluation of the loss of mass as a function of temperature. Fig.2.a and Fig.2.b represent the thermograms giving the variation of the mass loss (TG) and mass loss rate (DTG) as a function of the temperature of olive pomace flour before and after treatment at irradiation doses of 10 and 70 kGy [1].

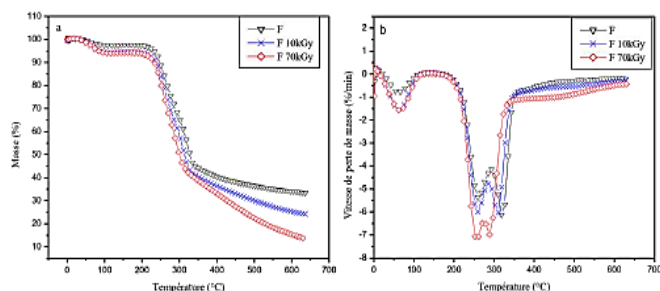


Figure 2. The thermograms: a) TG of untreated and treated F, b) DTG of untreated and treated F.

According to fig. 2.a, the thermograms of the mass loss (TG) of the treated and untreated olive pomace flour show the appearance of a mass loss around 65 and 68 °C, attributed to water evaporation [3]. After this temperature, the two flours are thermally stable up to 216°C, where the temperature at which the untreated or treated flour begins to decompose is recorded and this informs us that the irradiation has no effect on the temperature at which olive pomace flour begins to decompose.

In the temperature range between 216 ° C and 335 ° C, a significant loss of mass was observed and which is attributed to the degradation of hemicellulose, it is of the order of 50%, 51.7% and 50.6% for F, F10kGy and F70kGy respectively. Hemicellulose is the least stable constituent, it begins to decompose at 225°C and degrades at 325°C [4].

After 335°C, a second phenomenon of less significant mass loss was observed, it is due to the degradation of cellulose and lignin [5]. 13%, 19% and 28.35% are recorded for F, F10kGy and F70kGy respectively. Lignin begins to decompose before cellulose (200°C compared to 375 for cellulose), but its rate of decomposition is slower than cellulose and it is the last component to completely degrade [4].

The residue rate tends to decrease for irradiated flour, it goes from 33% for F to 24 and 13% for F10kGy and F70kGy respectively.

As indicated in the literature, the carbonization yield is proportional to the degradation of cellulose and increases if the structure degrades and becomes less crystalline [6]. In our case, the amount of carbon content tends to decrease, emphasizing that the starting material subjected to thermal analysis becomes more resistant to the increase in absorbed dose.

The three phases of mass loss discussed previously, manifested as peaks in mass loss rate (DGT) thermograms Fig 2.b. These peaks correspond to the maximum mass loss rate values.

The first peak located between 60 and 66°C corresponds to water evaporation. It is noted that the water evaporation rate is higher for the irradiated flour compared to the non-irradiated flour. 0.77, 1.54 and 1.56%/min are recorded at temperatures of 66, 64 and 62°C for F, F10kGy and F70kGy respectively.

The second peak located between 258 and 262 °C corresponds to the decomposition of hemicellulose and to the glycedic bonds of cellulose [7]. 5%, 6% and 7%/min are noted at temperatures of 259, 260 and 261°C for F, F10kGy and F70kGy respectively.

The third peak, which is between 260 and 320°C, is attributed to the decomposition of cellulose and lignin [8]. 6.12%, 6% and 7%/min are recorded at temperatures of 318, 311 and 288.5°C for F, F10kGy and F70kGy respectively.

It is noted that gamma irradiation at low doses, namely 10 and 70 kGy, slightly increases the rate of degradation of olive

pomace flour and it can also be concluded that cellulose and lignin are less sensitive to gamma irradiation than hemicellulose.

### C. Study of the biodegradation of irradiated composite materials by optical microscope

As it is important to know the morphology of the olive pomace flour used as filler in the PVC matrix, we used optical microscope imaging. Fig. 5 represents the images of F0 obtained by the optical microscope at different immersion times.

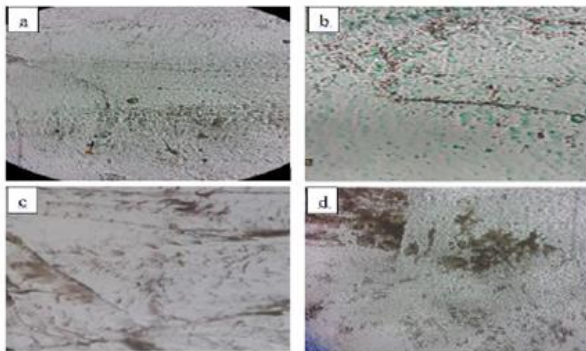


**Figure 3.** Morphology of F0 obtained by optical microscopy: a) before subsoil immersion, b) after 15 days of immersion, c) after 45 days of immersion, d) after 75 days of immersion.

According to this figure, we notice a change in the aspect of the different images obtained for the PVC, according to immersion time, this change and probably due to the possibility of migration or reaction of its additives with the medium where they are introduced.

Fig.4 represents the images of F20 obtained by the optical microscope at different immersion times.

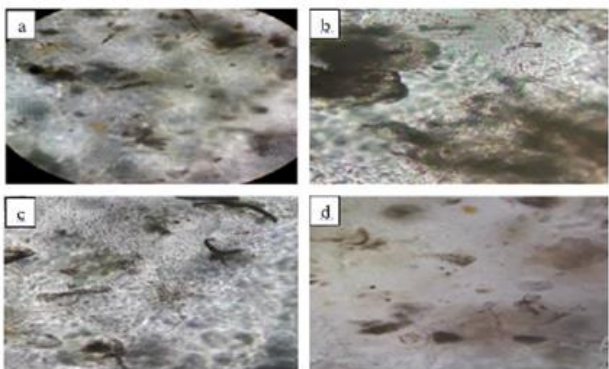


**Figure 4.** Morphology of F20 obtained by optical microscopy: a) before immersion basement, b) after 15 days of immersion, c) after 45 days of immersion, d) after 75 days of immersion.

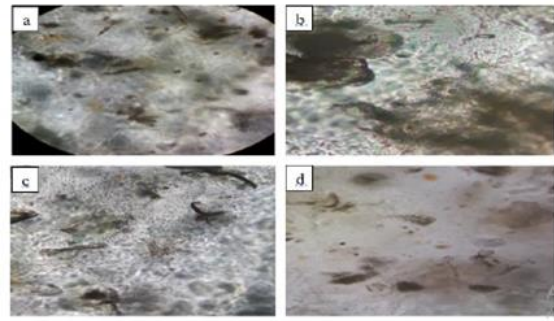


**Figure 5.** Morphology of F20 obtained by optical microscopy: a) before immersion

During the comparison, between the two fig.4, and 5 which are, accustomed to F0 and F20 successively, we notice for F0 that it has a single regular layer, and does not contains only additives, while for F20, we note that, it is made up of two layers which are the reinforcement and the matrix, this multilayer is due to the incompatibility between the two phases, where the structure appears in the form of conglomerates of olive pomace flour partially dispersed in the PVC matrix.

By comparing the images of F20 at different immersion times, we notice the increase in the size of the agglomerates. This increase is due to the swelling of the particles of the filler after the absorption of water due to rainfall precipitation during this period.

After 45 and 75 days, the images of the composites show the progressive reduction in the size of the agglomerates over time, due to the subtraction of the water previously absorbed, under the effect of the climatic heat.

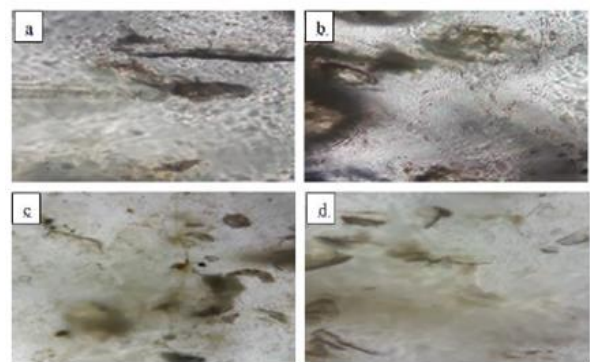


**Figure 6.** Morphology of F20CH10KGy obtained by optical microscopy: a) before subsoil immersion, b) after 15 days of immersion, c) after 45 days of immersion, d) after 75 days of immersion.

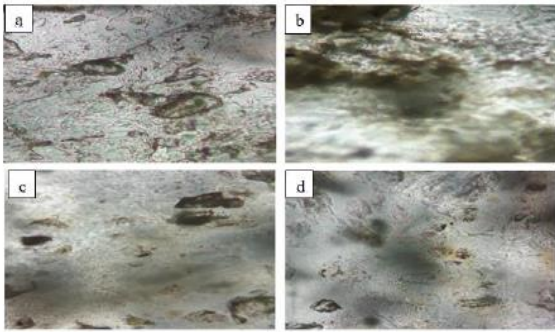


**Figure 7.** Morphology of F20CH25KGy obtained by optical microscopy: a) before subsoil immersion, b) After 15 days of immersion, c) After 45 days of immersion, d) After 75 days of immersion.

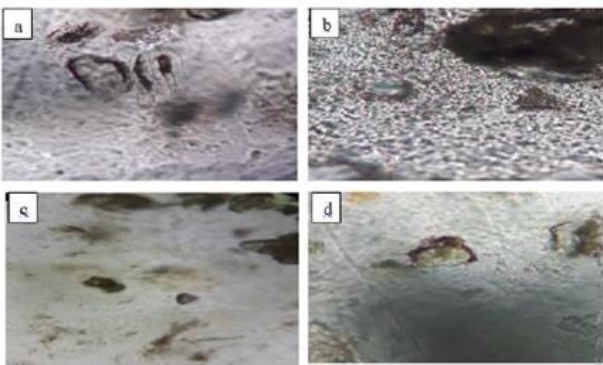


**Figure 8.** Morphology of F20CH50KGy obtained by optical microscopy: a) before subsoil immersion, b) after 15 days of immersion, c) after 45 days of immersion, d) after 75 days of immersion.

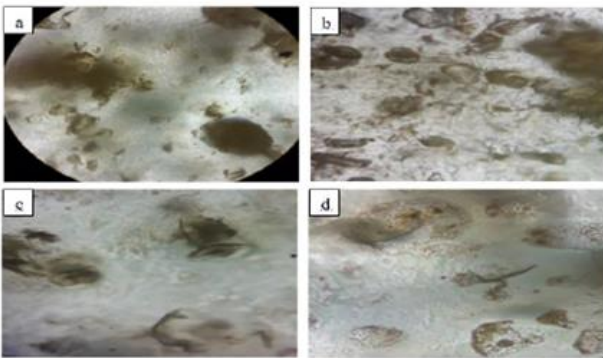


**Figure 9.** Morphology of F20CH60KGy obtained by optical microscopy: a) before subsoil immersion, b) after 15 days of immersion, c) after 45 days of immersion, d) after 75 days of immersion

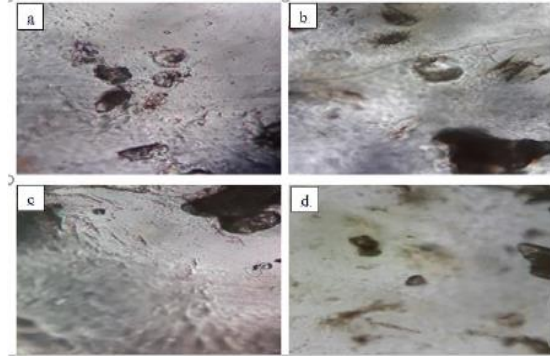


**Figure 10.** Morphology of F20CH70KGy obtained by optical microscopy: a) before subsoil immersion, b) after 15 days of immersion, c) after 45 days of immersion, d) after 75 days of immersion.

By analyzing the fig. from 6 to 10, we notice a change in the size of the olive pomace flour agglomerates after 15 days of immersion of the samples in the basement thanks to the absorption of humidity.

After 45 days of immersion of the samples underground, the figures indicate that the sizes of these agglomerates have decreased and that their compaction is less.

The same observation was recorded after 75 days, where it is found that the olive pomace flour particles have become fully spaced and less dense. This dispersion is further improved by increasing the dose of the irradiation. It can be seen that the treatment by gamma irradiation leads to good dispersion of the filler and better adhesion with the matrix.

In addition, the decrease in agglomerates can be attributed, to the decomposition of particles of olive pomace flour under the influence of certain environmental factors such as PH, microorganisms and other factors, which leads to the biodegradation of composite materials.

**D. Study of the biodegradation of irradiated composite materials by optical microscope the measure of the Mass loss**

**Fig. 11** represents the variation in mass loss of F0 and F20 as a function of immersion time.

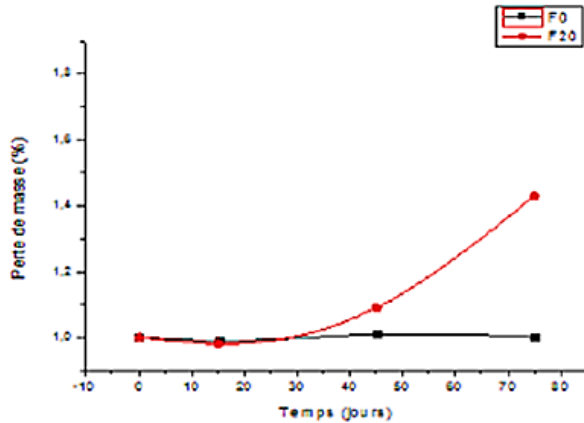


**Figure 11.** The variation of mass loss of F0 and F20 as a function of immersion time.

From this curve, we clearly see the absence of mass loss of F0, which is evident for polymeric materials that have a long life. We note the increase in mass loss of F20, by increasing the immersion time.

This mass loss is mainly due to the biodegradation of the filler presented in the PVC matrix. Figure.15 represents the variation in mass loss of F20, F20CH10KGy, F20CH25KGy, F20CH50KGy, F20CH60KGy and F20CH70KGy as a function of immersion time.

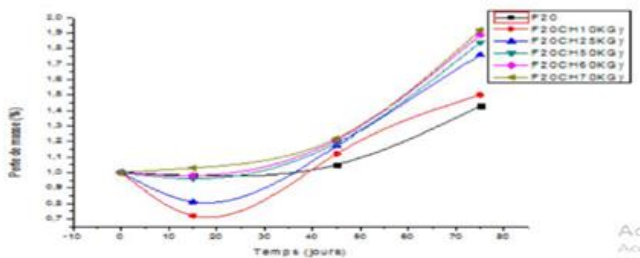


**Figure 12.** Curve represents the variation in mass loss of F20, F20CH10KGy, F20CH25KGy, F20CH50KGy, F20CH60KGy and F20CH70KGy

In this figure, we notice that the mass increased during the first 15 days for all the samples. We explained this increase by the amount of water absorbed by the hydrophilic reinforcement, which led to the swelling of its particles.

The composites reinforced by the irradiated filler show a greater mass loss compared to the composites loaded with the non-irradiated olive pomace flour. This mass loss became more important by increasing the radiation dose. It can be concluded that the treatment with gamma irradiation contributed to the biodegradation of composites.

## V. Conclusion

The study carried out in this work aimed at the influence of natural fibers on the characteristics of PVC-based composites

and olive pomace flour. The problem of the absence of adhesion between the PVC matrix and the olive pomace flour reinforcement has been treated and improved by low-dose gamma irradiation. The filler remained thermally stable and its particle size was reduced and well dispersed.

The study of the biodegradability of the composites developed has allowed us to conclude that the addition of vegetable fibers in a thermoplastic matrix is an effective solution to obtain a biodegradable composite material which decomposes naturally when it is in contact with various environmental factors.

This conclusion is confirmed by the photos taken by the optical microscope, where the reduction in the size of the agglomerates was observed with a dispersion of the FGO. The decomposition of composites is evidenced by their loss of mass.

## References:

1. N. Bellili, Elaboration et caractérisation des composites a base d'une matrice thermoplastique chargée avec des fibres, Université de Bejaia, 2015.
2. A.K. Bhowmick, S. Ray, K.S.S. Sarma, A.B. Majali, V.K. Tikku, Characterization of electron-beam-modified surface coated clay fillers and their influence on physical properties of rubbers, Radiation Physics and Chemistry, 65, 2002.
3. S.N. Monteiro, V. Calado, R.J.S. Rodriguez, F.M. Margem, Thermogravimetric stability of polymer composites reinforced with less common lignocellulosic fibers – an Overview, Journal of Materials Research and Technology, 1(2), 2012.
4. S.Wang, O. Hosseinaei, A.A. Enayati, T.G. Rials, Effects of hemicellulose extraction on properties of wood flour and wood-plastic composites, Composites : Part A 43, 2012.
5. H. Djidjelli, A. Boukerrou, A. Rabouhi, R. Founas, M. Kaci, O. Zefouni, N. Djillali, L.Belmouhoub, Effect of olive residue Benzylolation on the thermal and mechanical properties of poly(vinyl chloride)/olive residue composites, Journal of Applied Polymer Science, 107, 2008.
6. A. Cemmi, S. Baccaro, M. Carewska, C. Casieri, A. Lepore, Structure modifications and interaction with moisture in g-irradiated pure cellulose by thermal analysis and infrared spectroscopy, Polymer Degradation and Stability, 98, 2013.
7. M. Pracella, D. Chionna, I. Anguillesi, Z. Kulinski, E. Piorowska, Functionalization, compatibilization and properties of polypropylene composites with

- hemp fibers. *Composites Science and Technology*, 66, 2006.
8. A. Boukerrou, S. Krim, H. Djidjelli, C. Ihamouchen, J. Martinez, J. Juan, Study and characterization of composites materials based on polypropylene loaded with olive husk flour, *Journal of Applied Polymer Science*, 122, 2011.

# Preparation and characterization of Polypropylene /Polyethylenterephthalate/wood Fibers composites in the presence of compatibilizer

Badrina DAIRI <sup>1,2</sup> \* ;Nadira BELLILI <sup>1,2</sup> ; Hocine DJIDJELLI <sup>2</sup>; Amar BOUKERROU<sup>2</sup>

*1*Department of Process Engineering, Faculty of Technology, Skikda University 20 August – 1955 – Algeria.

*2* Department of Process Engineering, Faculty of Technology, Laboratory of Advanced. Polymer Materials (LMPA), Abderrahmane MIRA University, Béjaïa 06000, Algeria.

\*Corresponding author: [b.dairi@univ-skikda.dz](mailto:b.dairi@univ-skikda.dz) or [badrina\\_d@yahoo.fr](mailto:badrina_d@yahoo.fr)

Received: 8 May 2023; Accepted: 27 July 2023, Published : 29 July 2023

## Abstract

*This work consists in studying the structure-property relationships of polymer blends based on recycled polypropylene (PP) and poly (ethylene terephthalate). This research reports the results of incorporating a vegetable filler into the PP / r-PET blend. A synergistic effect is observed during the simultaneous incorporation of the wood flour and the agent compatibilizing MAPP in the polymer mixture. Composites based on PP / r -PET was prepared in two steps. Scanning electron microscopy (SEM) analysis of the fractured surface samples revealed a better interaction between the WF and the polymer mixture. The thermogravimetric analysis (ATG / DTG) of the sample showed that the presence of the filler decreases the thermal stability of the composites compared to the PP / r -PET mixture, but does not accelerate the degradation process. The DSC allows showing that the incorporation of wood flour in the mixture of polymer PP / PET-r has an influence on the values of  $T_f$  of the two polymers (PP and r -PET), with an increase in the degree of crystallinity was observed.*

**Keywords:** Polypropylene, Polyethylene terephthalate, Wood flour, Composite materials, Thermal properties.

## I. Introduction

A recent notion (which is taken more and more into account in our daily life) is the notion of sustainable development, depending in part on waste reduction and / or their management. This involves their treatment with a view to their recovery or their recycling. A large part of the waste consists of plastics used in convenience products, household appliances, construction, transport, etc.

Unfortunately, plastics, in general, have a major drawback, which is their resistance to biodegradation. One of the possible solutions to reduce them or eliminating them is recycling. This can be mechanical or chemical. Mechanical recycling consists of reusing waste for the manufacture of a finished or semi-finished material. However, this type of recycling generally results in the decrease in polymer properties. Among these plastics, poly (ethylene terephthalate) (PET) is considered one of the most important technical polymers.

PET is mainly used for the manufacture of films, fibers and containers (bottles). PET has very good characteristics for its use in packaging: high transparency in blown containers, good mechanical properties for minimum thickness, dimensional stability during handling (even at high temperatures),

relatively low cost (price per container) and low permeability to gases such as CO<sub>2</sub> [1]. For all these reasons, PET is increasingly used as packaging material. Its widespread use generates significant quantities of waste that require the implementation of recycling techniques.

Recycling PET is not easy because of its degradation during reprocessing, caused by temperature, humidity and contaminants. Degradation, leads to decrease in molecular weight and loss of properties [2]. A way to improve the properties of recycled polymers is to mix them with polymers not modified (polyolefin) with good properties.

Polypropylene (PP) is widely used in this case [3], because of its good properties (lightness, transparency, high mechanical resistance, electrical insulation, inertia to chemical aggression and use at high temperatures) [4]. It has been reported that mixtures of polyolefin (especially polyethylene (PE) and PP) and PET can display good mechanical characteristics and of permeability.

However, PET and polyolefin have very different strong chemical structures. , which makes them immiscible with each other. The major drawback resulting from this incompatibility is that the resulting mixtures exhibit mechanical properties

mediocre. The most frequently used means of partially filling this deficit performance is the compatibilization, which consists in, creating chemical affinities between constituents of the mixture in order to reduce interfacial tensions, improve adhesion between phases and stabilize morphology [5]. Some of these studies have focused on the techniques to improve the compatibility between the two polymers [6, 7]. PP grafted with anhydride maleic (MAPP) can be used as a compatibilizer in mixtures of PP / PET-r [8- 11]. The strengthening of polymeric materials is expressed by the improvement of certain processing and end-use properties.

The last few decades have seen an interest growing for the use of renewable resources as back-ups in systems composite polymers. This is due to the growth of environmental regulations and increased interest in the proper use of renewable natural resources for develop environmentally friendly materials. In this way, the incorporation of natural fibers, especially wood flour as a reinforcing filler, can produce composites which often exhibit a remarkable improvement in their properties, for example compared to the pure polymer. Indeed, the addition of wood flour as a natural filler renewable in polymer blends aims to produce a unique combination of high performance, lightness, recyclability, biodegradability and the advantages of low cost processing.

The incorporation of wood flour in such a matrix polymer blend can lead to the development of a new group of materials composites. These advantages have led to the use of natural fillers such as, potential replacement for traditional reinforcement materials such as fiberglass, calcium carbonate and silica in composite systems [12]. However, there are certain limits to their use for structural applications. The main problem stems from the inherent incompatibility of most polymer matrices due to the high cellulose content of natural fibers.

The presence of polar hydroxyl groups (-OH) on lignocellulosic material leads to a hydrophilic character of these fibers, which weakens the interfacial bond with the hydrophobic organic matrices [13]. The poor compatibility between the two phases leads to poor interaction and therefore low capacity of the matrix to transfer charges applied to the reinforcing fibers. To solve the problem, the maleated polyolefins are commonly used as coupling agents to establish a good interaction between each phase in the composite [14]. Several studies have been carried out on the production of composites of natural fibers based on polyolefin blends (PP / PE) [15-20], however, little work has focused on polyolefin / recycled PET as a matrix [21, 22].

## II. Material and methods

PP 500P polypropylene with a melt flow index of 3.00 g/10 min was provided by SABIC Basic Industries Corporation (Saudi Arabia). Poly(ethylene terephthalate) (r-PET), or waste r- PET, was recovered from waste mineral water bottles. The size of r-PET pieces ranged from 2 to 5 mm. Maleic anhydride-

grafted-polypropylene (MAPP) with a melt flow index of 2.63 g/10 min was provided by Arkema (Insa de Lyon, France). The WF was extracted from Aleppo pine trees growing in the Djelfa region in southern Algeria. Average particle size was approximately 50  $\mu$ m.

**Table 1:** Formulations of PP/r-PET/WF composites

Sample	PP (wt %)	r -PET (wt%)	MAPP (wt%)	Wood flour (wt%)
PP/r-PET/WF10	70	20	0	10
PP/r-PET/WF20	60	20	0	20
PP/r-PET/WF30	50	20	0	30
PP/r-PET/WF10C	60	20	10	10
PP/r-PET/WF20C	50	20	10	20
PP/r-PET/WF30C	40	20	10	30

The r-PET was dried at 120°C, WF at 105°C, and PP and MAPP at 90°C. The composites were produced in a two-stage process: (i) extrusion for pelletizing and (ii) injection molding. In the first stage, the PP/r-PET blend (matrix) was extruded at the melting temperature of PET at 265°C and 120 rpm for 2 min using a laboratory scale co-rotating twin-screw mini extruder (15 mL Micro compounder, DSM Xplore, University A. Mira of Bejaia, Algeria). After air cooling, the extrudates were cut into pellets. In the second stage, composites were produced in the presence or absence of MAPP at 10%, 20%, and 30% WF content. The PP/r-PET pellets, WF and 10% MAPP compatibilizer [23–25] were mixed and fed into the same twin screw extruder at 180°C and 100 rpm for 10 min to prevent degradation of the cellulose fibers. Compounding ratios of the prepared composites are presented in Table 1. The compounds were subsequently injection molded using a laboratory scale injection molding machine (12 mL Micro injection Molder, DSM Xplore, University A. Mira of Bejaia, Algeria) at 180°C barrel temperature, 90°C mold temperature, and 10 bars injection and holding pressure. Samples were molded for mechanical and physical characterization.

Sample morphology was performed on Hitachi S- 3500N Variable Pressure Scanning Electron Microscope (Hitachi High Technologies Canada) with an accelerating voltage of 20.0 kV. Specimens were freeze-fractured in liquid nitrogen and then coated with a thin layer of carbon for characterization.

In thermogravimetric analysis (TGA), the mass of a sample, maintained in controlled atmosphere, is recorded as a function of the temperature (rise, fall isothermal) or time. Saved thermograms provide information mainly on the physical phenomena of vaporization, sublimation or desorption, but also on decomposition or oxidation reactions, particularly in the case of polymers [26].

In this study we used a TGA Q500 type device from TA instruments. He is composed of a sample boat driven by a high

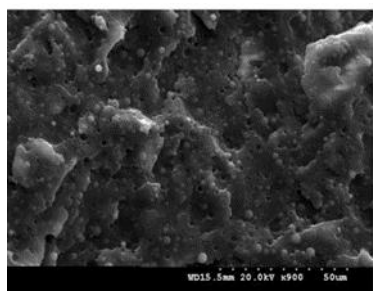
precision microbalance. The basket is introduced into an oven allowing the sample to be subjected to a ramp in temperature from 20 to 600 °C with a speed of 10 °C/ min, under a flow of inert gas (N<sub>2</sub>).

The characterization of crystallization and melting of polymers can be carried out by considering the thermal exchanges linked to these processes. In fact, heat is released when the polymer crystallizes as it absorbs heat as it melts. Analysis Differential Scanning Calorimetry (DSC) is used to measure the amounts of heat released or absorbed during these steps, by applying the same temperature program to, the tested sample and an inert reference. A signal proportional to the power difference, supplied to the sample and to the reference (dw / dt) is recorded [27].

This method is widely used for the characterization of polymers. It provides information on the glass transition of amorphous polymers, temperature and enthalpies melting and crystallization of semi- crystalline polymers .She permits, in particular, to follow the evolution of crystallinity through the estimation of the crystallinity rate [28].

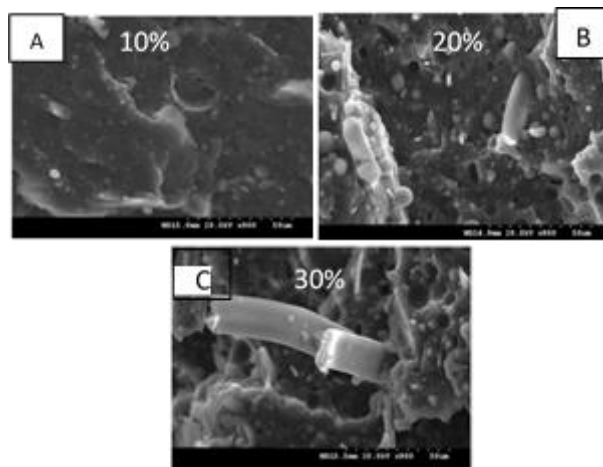
### III. Results and discussion

Figure 1 shows the SEM micrograph of the rupture surface of the PP / PET-r mixture (80/20). It can be seen that PET-r is dispersed in the continuous phase of PP, in the form of globular particles. The fractured surface has many voids, and the interface between the r-PET particles and the continuous phase of PP can be clearly distinguished, indicating the immiscibility of both r-PET and PP polymers.



**Figure 1:** SEM micrograph of the mixture of PP/r-PET (80/20).

Adding 10, 20 and 30% of the cellulosic filler to the PP / r-PET mixture causes the onset of distinct phases, as shown in Figure 2. It seems that no interaction has developed between the phases, which reveal a weak affinity between wood flour and polymer blend (PP / r-PET). The morphology of surface shows a rough, irregular and heterogeneous surface as well as the presence of micro voids and cavities on the surface due to the release of the load from the matrix PP / r -PET during fracture. These micro voids become more pronounced as the rate of load increases (Figures B and C), highlighting the incompatibility of the phases due to the poor interfacial adhesion between the WF and the PP /r- PET mixture.



**Figure 2:** SEM micrograph of the composite of PP/r-PET/ WF, in the absence of MAPP.

Figure 3 show the micrographs, respectively, of composites PP /r -PET/ WF10C, PP/r -PET/WF20C and PP /r -PET / WF30C.

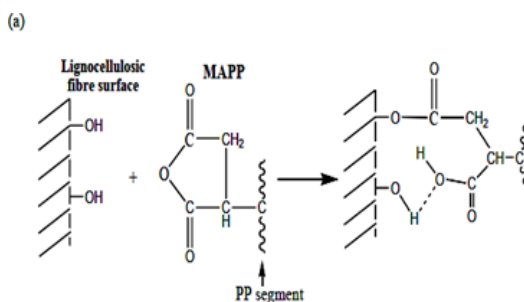
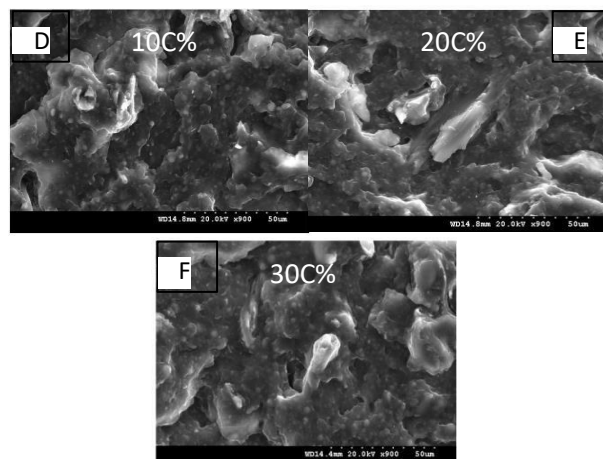


**Figure 3:** SEM micrograph of the composite of PP / r -PET / WF10C/20C/30C, in the presence of MAPP.

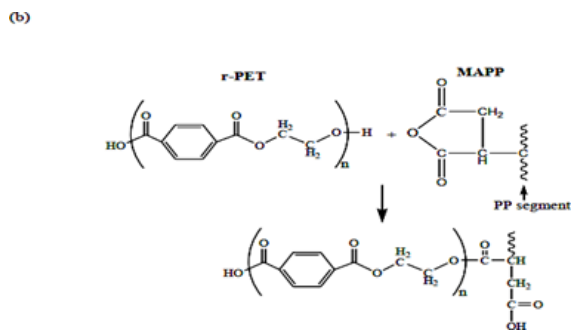


Figure 4: Chemical reactions between: Lignocellulosic loads and MAPP r -PET and MAPP.

The presence of a compatibilizer considerably modifies the morphology of the composite. The incorporation of the copolymer of MAPP (at 10%) as a compatibilizer, results in a more homogeneous and smooth surface with less cavities and microvoids, in comparison with that of non- compatibilized composites. Indeed, the micrographs show better adhesion between the cellulosic filler and the mixture of polymer resulting from the reduction of the interfacial tension between the components. This is attributed to the ability of MAPP to interact with both polypropylene, poly (ethylene terephthalate) and wood flour. The proposed coupling mechanism is a binding hydrogen and the covalent bond of the ester produced by the chemical reaction of anhydride groups of MAPP and hydroxyl groups on the surface of fibers [29, 30] and also the chemical reaction between maleic anhydride and terminal functional groups PET-r as shown in Figure 4. The chemical reaction between the anhydride maleic (AM) and the -OH groups of PET-r resulted in a PP-g-PET copolymer during melting the mixture [31]. The use of MAPP in the composite has a pronounced effect on the creation of interactions between the components present in the composites [32].

### Thermal properties:

#### Thermogravimetric analysis (TGA)

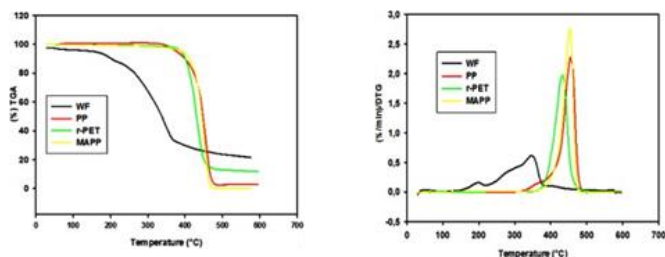


Figure 5: ATG/DTG thermograms of Wood Flour (WF), PP, r-PET and MAPP.

From the ATG thermograms (Figure 5), it can be seen that PP, PET-r and MAPP decompose in a single step, and that the temperatures at the start of degradation ( $T_{\text{degradation 5\%}}$ ) are 377.68°C, 389.46 °C and 391.91 °C, respectively. The latter (MAPP) exhibits high thermal stability compared to that of PP, PET-r and cellulosic filler. Conversely, wood flour has three stages of decomposition. The first at 100 °C is attributed to the gradual evaporation of the absorbed water. From 200 °C to 350 °C, there is degradation of hemicellulose and above 350 °C; it is associated with decomposition and condensation of aromatic rings in lignin [33].

Figure 6 represent the ATG and DTG thermograms of the composites not compatible with PP / r -PET / WF at different loading rates (10, 20 and 30%).

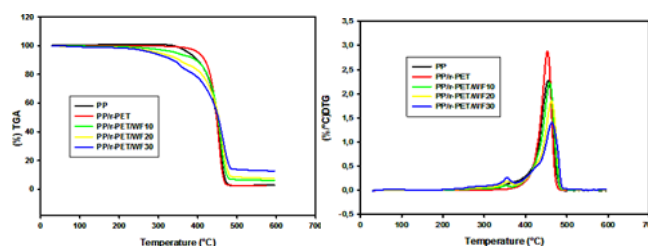


Figure 6: ATG/ DTG thermograms of PP / r -PET and PP / PET-r / WF composites, in absence of MAPP.

From the ATG thermograms shown in Figure 6, we observe that the Thermal degradation profiles of incompatible composites are similar. Indeed, we record three stages of degradation for composites, while we observe that a single decomposition stage for the polypropylene /poly (ethylene terephthalate) recycled. We note that the incorporation of wood flour in the PP / PET-r mixture decreases the temperature of the onset of decomposition and this decrease is greater than the charge rate increases. It is estimated at 402.55 °C for PP / r -PET, 347.25 °C, 301.78 °C and 285.61 °C for non-compatibilized composites PP/r-PET / WF10, PP / r -PET / WF20 and PP / r - PET / WF30, respectively. This decrease can be attributed to the presence of the three main constituents (cellulose, hemicellulose and lignin) of the cellulose filler [34]. The cellulosic filler degrades between 200 °C and 350 °C. While our polymer blend PP/r-PET degrades at temperatures above 400 °C. Therefore the thermal behavior of the composite represents the sum of the individual behaviors of these constituents, lignocellulosic filler and mixture of PP / r -PET. Around of 485 °C, a level of stability is recorded, attributed to the formation of ash However, looking at the peaks of the DTG thermograms shown in Figure 6,

It is noted that the temperatures corresponding to the maximum speeds of degradation recorded are : 458.33 °C, 461.25 °C and 464.70 °C for the non- compatibilized PP/r-PET/WF composites at different loading rates, 10%, 20% and 30%, respectively, which are

significantly higher than that of the PP / r -PET mixture which is 454.36 °C. Apart from the initial decomposition temperature, it can be clearly seen that the charge Lignocellulosic significantly retards the degradation of the PP / r - PET mixture. In other words, it acts as an inhibitor of thermal degradation.

The effect of the compatibilizer on the thermal behavior of composites PP / r -PET / WF is shown in Figure 7.

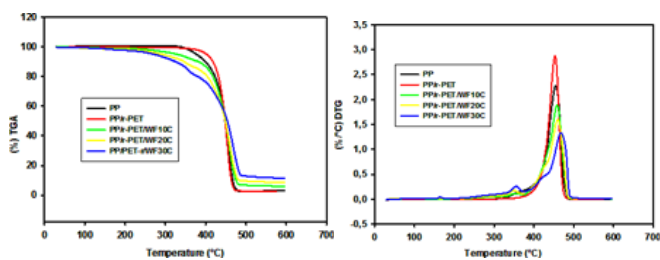


**Figure 7:** ATG/DTG thermograms of PP / r - PET and PP / PET-r / WF composites, in presence of MAPP.

In the presence of MAPP in PP / PET-r / WF composites at different loading rates (10%, 20% and 30% by weight), the temperatures corresponding to the maximum speeds of degradations ( $T_{\text{to } V_{\text{max}}}$ ) are shifted to higher temperatures compared to those of non- compatibilized composites.

The improvement in the thermal stability of compatibilized composites is due to better interfacial adhesion and over intermolecular bonds which produces a reaction esterification between the hydroxyl groups of the lignocellulosic charge and the maleic anhydride functional group of MAPP [35, 36].

This result indicated that the use of a compatibilizer in composite systems improves the thermal stability of composites [37-40]. However, composites not compatibilized were easily thermally degraded by the increase in temperature which is due to poor interfacial adhesion between the polymer mixtures PP / r-PET and wood flour which degrades the thermal properties of the materials of composites [41, 42].

#### Differential Scanning Calorimetry (DSC):

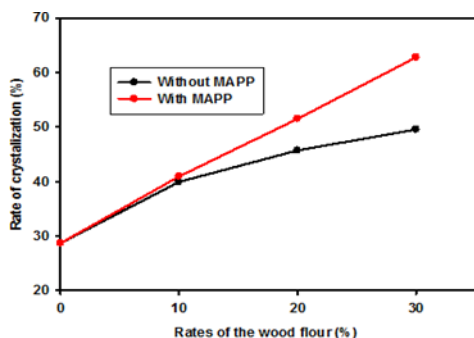


**Figure 8:** Evolution of the crystallinity rate of PP / r-PET

/ WF composites, in the absence and in the presence of MAPP.

From the results obtained, it can be seen that the introduction of WF into the mixture of PP/r-PET increases the crystallinity rate (Figure 8), the latter increase as the flour rate increases. It goes from 28.70% for the; mixture (matrix) PP / r - PET pure at 39.93% for the composite PP / r-PET / WF10 at 10% and 45.70% for the PP / r-PET / WF20 composite at 20% and 49.54% for the PP / r - PET composite at 30%, respectively. Generally, the incorporation of the cellulosic filler into the matrix polymeric occurs in the amorphous zone of the material and the surface of the filler acts as nucleation sites which modify the crystallization kinetics of polymers [48, 49]. The presence of wood flour in the PP / r -PET mixture decreases the  $T_f$  of PP and PET-r by compared to the pure PP / PET-r mixture, there is therefore the formation of crystals of smaller size or with more flaws. For compatibilized composites, the DSC data reported in Table 3 determine that the degree of crystallinity is higher than that of non-composite composites compatible with different charge rates. According to the literature, this could be due to stronger interactions between the lignocellulosic charges (WF) and the polymer mixture. PP /r-PET is affected by maleic anhydride moieties containing agent-compatibilizing MAPP. The influence of charge on the crystallization of PP and r-PET would then be larger. A similar effect was observed by Luz et al. [44].

#### I. Conclusions

An innovative composite material based on wood flour and a polymer blend PP /r-PET was developed using two extrusion cycles, followed by molding by injection. The effect of the addition of wood flour (WF) as well as the compatibilizer MAPP on the morphology and thermal properties of PP / r -PET / WF composites was studied. Scanning electron microscopy (SEM) of PP / r-PET / WF composites has indicated that the addition of MAPP had beneficial effects on the compatibilized PP / r-PET / WFC composites, resulting in a homogeneous load distribution (WF) and a strong adhesion between the filler and the PP / r - PET mixture.

Thermogravimetric analysis (ATG / DTG) of the samples reveals that the presence of the load at different contents (10, 20 and 30%), decreases the thermal stability of composites compared to PP / r - PET blend, but does not accelerate the degradation process. However, with the addition of MAPP an improvement in the thermal stability of composites is recorded.

The differential calorimetric analysis shows that the incorporation of the wood flour in the polymer mixture PP / r-PET has an influence on the values of melting temperatures of the two polymers (PP and r-PET), with an increase in the rate of crystallinity is observed. The surface of the flour acts as nucleation sites which modifies the crystallization kinetics of PP and r -PET.

All these results obtained allow us to conclude that the presence of wood and the compatibilizer MAPP has a strengthening effect of the PP / r-PET mixture. This technology offers a way to use engineering plastics (r-PET) for applications of WPC (Wood Plastic Composite).

## References

- [1] C. TAN, I. AHMAD, M. HENG, «*Characterization of polyester composites from recycled polyethylene terephthalate reinforced with empty fruit bunch fibers*», *Materials and Design*, 32, 4493–4501, (2011).
- [2] N.G. KARSLI, S. YESIL, A. AYTAC, «*Effect of short fiber reinforcement on the properties of recycled poly (ethylene terephthalate)/poly(ethylene naphthalate) blends*», *Materials and Design*, 46, 867–872, (2013).
- [3] Y.X. PANG, D.M. JIA, H.J. HU, D.J. HOURSTON, M. SONG, «*Effects of a compatibilizing agent on the morphology, interface and mechanical behaviour of polypropylene/poly(ethylene terephthalate) blends*», *Polymer*, 41, 357–365, (2000).
- [4] M. KACI, A. HAMMA, I. PILLIN, Y. GROHENS, «*Effect of Reprocessing Cycles on the Morphology and Properties of Poly(propylene)/Wood Flour Composites Compatibilized with EBAGMA Terpolymer*», *Macromolecular Materials and Engineering*, 294, 532–540, (2009).
- [5] P. VAN PUYVELDE, S. VELANKAR, P. MOLDENAERS, «*Rheology and morphology of compatibilized polymer blends*», *Current Opinion in Colloid and Interface Science*, 6, 457–463, (2001).
- [6] M.F. CHAMPAGNE, M. A. HUNEALULT, C. ROUX, W. PEYREL, «*Reactive compatibilization of polyethylene terephthalate/polypropylene blends*», *Polymer Engineering and Science*, 39, 976–984, (1999).
- [7] C.P. PAPADOPOULOU, N.K. KALFOGLOU, «*Comparison of compatibilizer effectiveness for PET/PP blends: their mechanical, thermal and morphology characterization*», *Polymer*, 41, 2543–2555, (2000).
- [8] K.H. YOON, H.W. LEE, O.O. PARK, «*Properties of poly(ethylene terephthalate) and maleic anhydride-grafted polypropylene blends by reactive processing*», *Journal of Applied Polymer Science*, 70, 389–395, (1998).
- [9] Y.X. PANG, D.M. JIA, H.J. HU, D.J. HOURSTON, M. SONG, «*Effects of a compatibilizing agent on the morphology, interface and mechanical behaviour of polypropylene/poly(ethylene terephthalate) blends*», *Polymer*, 41, 357–365, (2000).
- [10] M.K. CHEUNG, D. CHEN, «*Mechanical and rheological properties of poly(ethylene terephthalate)/polypropylene blends*», *Polymer International*, 43, 281–287, (1997).
- [11] M. XANTHOS, M.W. YOUNG, J.A. BIESENBERGER, «*Polypropylene/polyethylene terephthalate blends compatibilized through functionalization*», *Polymer Engineering and Science*, 30, 355–365, (1990).
- [12] H.D. ROZMAN, G.S. TAY, R. N. KUMAR, A. ABUSAMAH, H. ISMAIL, «*Polypropylene-oil palm empty fruit bunch-glass fiber hybrid composites: A preliminary study on the flexural and tensile properties*», *European Polymer Journal*, 37, 1283–1291, (2001).
- [13] D.B. DITTENBER, H.V.S. GANGARAO, «*Critical review of recent publications on use of natural composites in infrastructure*», *Composites Part A: Applied Science and Manufacturing*, 43, 1419–1429, (2012).
- [14] T.J. KEENER, R.K. STUART, T.K. BROWN, «*Maleated coupling agents for natural fiber composites*», *Compos Part A: Applied Science and Manufacturing*, 35, 357–362, (2004).
- [15] C. CLEMONS, «*Elastomer modified polypropylene- polyethylene blends as matrices for wood flour-plastic composites*», *Compos Part A: Applied Science and Manufacturing*, 41, 1559–1569, (2010).
- [16] S.K. NAJAFI, E. HAMIDNIA, M. TAJVIDI, «*Mechanical properties of composites from sawdust and recycled plastics*», *Journal of Applied Polymer Science*, 100, 3641–3645, (2006).
- [17] N.T. DINTCHEVA, F.P. LA MANTIA, «*Recycling of the “light fraction” from municipal postconsumer plastics: Effect of adding wood fibers*», *Polymers for Advanced Technologies*, 10, 607–614, (1999).
- [18] N.T. DINTCH VA, F.P. LA MANTIA, F. TROTTA, M.P. LUDA, G. CAMINO, M. PACI, L. DI MAIO, D. ACIERNO, «*Effects of filler type and processing apparatus on the properties of the recycled “light fraction” from municipal post-consumer plastics*», *Polymers for Advanced Technologies*, 12, 552–560, (2001).
- [19] M. TASDEMIR, H. BILTEKIN, G.T. CANEBA, «*Preparation and characterization of LDPE and PP-Wood fiber composites*», *Journal of Applied Polymer Science*, 112, 3095–3102, (2009).
- [20] Y. CUI, S. LEE, B. NORUZIAAN, M. CHEUNG, J. TAO, «*Fabrication and interfacial modification of wood/recycled plastic composite materials*», *Compos Part A: Applied Science and Manufacturing*, 39, 655–661, (2008).
- [21] Y. LEI, Q. WU, «*Wood plastic composites based on microfibrillar blends of high density polyethylene/poly(ethylene terephthalate)*», *Bioresource Technology*, 101, 3665–3671, (2010).
- [22] Y. LEI, Q. WU, «*High density polyethylene and poly (ethylene terephthalate) in situ submicro-fibril blends as a matrix for wood plastic composites*», *Composites Part A: Applied Science and Manufacturing*, 43, 73–78, (2012).
- [23] H. Zhang, W. Guo, Y. Yu, B. Li, and C. Wu, *Eur. Polym. J.*, 43, 3662 (2007).
- [24] K. Jarukumjorn and S. Chareunkun, *Suranaree J. Sci. Technol.*, 14, 1 (2007).
- [25] M. Kaci, A. Benhamida, S. Cimmino, C. Silvestre, and C. Carfagna, *Macromol. Mater. Eng.*, 290, 987 (2005).
- [26] D.A. SKOOG, F.J. HOLLER, T.A. NIEMAN, «*Principe d'analyse instrumentale*», 5ème Edition de Boeck, Paris, (2003).
- [27] S. DEVISME, «*Contribution à l'étude de l'extrusion couchage de polypropylène sur l'aluminium*», Thèse de Doctorat, Ecole des mines de Paris, (2006).
- [28] Z. AMALOU, «*Contribution à l'étude de la structure semi cristalline des polymères à chaînes semi rigides* », Thèse de Doctorat, Université Bruxelles, (2006).
- [29] I. NAGHMOUCHI, F.X. ESPINACH, P. MUTJÉ, S. BOUFI, «*Polypropylene composites based on lignocellulosic fillers: How the filler morphology affects the composite properties*», *Materials and Design*, 65, 454–461, (2015).
- [30] J.M. FELIX, P. GATENHOLM, «*The nature of adhesion in composites of modified cellulose fibers and polypropylene*», *Journal of Applied Polymer Science*, 42, 609–920, (1991).
- [31] Y. TAO, K. MAI, «*Non-isothermal crystallization and melting behavior of compatibilized polypropylene/recycled poly(ethylene terephthalate) blends*», *European Polymer Journal*, 43, 3538–3549, (2007).
- [32] S.M.B. NACHTIGALL, G.S. CERVEIRA, S.M.L. ROSA, «*New polymeric-coupling agent for polypropylene/wood-flour composites*», *Polymer Testing*, 26, 619–628, (2007).
- [33] A.J. NUMEZ, J.M. KENNY, M.M. REBOREDO, M.I. ARANGUREN, N.E. MARCOVICH, «*Thermal and Dynamic Mechanical Characterization of Polypropylene/Wood Flour composites* », *Polymer Engineering and Science*, 42, 733–741, (2002).
- [34] E. PÜTÜN, B.B. UZUN, A.E. PÜTÜN, «*Composition of products obtained via fast pyrolysis of olive-oil residue: Effect of pyrolysis temperature*», *Journal of Analytical and Applied Pyrolysis*, 79, 147–153, (2007).
- [35] S. MOHANTY, S.K. VERMA, S.K. NAYAK, «*Dynamic Mechanical and Thermal Properties of MAPE Treated Jute/HDPE Composites*», *Composites Science and Technology*, 66, 538–547, (2006).
- [36] H. HATAKEYEMA, N. TANAMACHI, H. MATSUMURA, S. HIROSE, T. HATAKEYAMA, «*Bio-based polyurethane composite foams*

- with inorganic fillers studied by thermogravimetry», *Thermochimica Acta*, 43, 155–160, (2005).
- [37] H. DEMIR, U. ATIKLER, D. BALKOSE, F. TIHMINLIOGLU, «The effect of fiber surface treatments on the tensile and water sorption properties of polypropylene-luffa fiber composites», *Composites Part A: Applied Sciences and Manufacturing*, 37, 447-45, (2006).
- [37] V. TSERKI, P. MATZINOS, S. KOKKOU, C. PANAYIOTOU, «Novel biodegradable composites based on treated lignocellulosic waste flour as filler. Part I. Surface chemical modification and characterization of waste flour», *Composites Part A: Applied Sciences and Manufacturing*, 36, 965-974, (2005).
- [38] D. HARPER, M. WOLCOTT, «Interaction between coupling agent and lubricants in wood–polypropylene composites», *Composites Part A: Applied Science and Manufacturing*, 35, 385-394, (2004).
- [39] S.M.B. NACHTIGALL, G.S. CERVEIRA, S.M.L. ROSA, «New polymeric-coupling agent for polypropylene/wood-flour composites», *Polymer Testing*, 26, 619–628, (2007).
- [40] H.S. YANG, M. WOLCOTT, H.S. KIM, H.J. KIM, «Thermal properties of lignocellulosic fiber-thermoplastic polymer bio composites», *Journal of Thermal Analysis and Calorimetry*, 82, 157–160, (2005).
- [41] S.H. MANSOUR, J.N. ASSAD, B.A. ISKANDER, S.Y. TTAWFIK, «Influence of some additives on the performance of WF/Polyolefin composite», *Journal of Applied Science*, 109, 2243-2249, (2008).
- [42] P.V. JOSEPH, K. JOSEPH, S. THOMAS, C.K.S. PILLAI, V.S. PRASAD, G. GROENINCKX, MARIANA SARKISSOVA, «The thermal and crystallisation studies short sisal fibre reinforced polypropylene composites», *Composites Part A: Applied Science and Manufacturing*, 34, 253-266, (2003).
- [43] P.V. JOSEPH, K. JOSEPH, S. THOMAS, C.K.S. PILLAI, V.S. PRASAD, G. GROENINCKX, MARIANA SARKISSOVA, «The thermal and crystallisation studies of short sisal fibre reinforced polypropylene composites», *Composites Part A: Applied Science and Manufacturing*, 34, 253-266, (2003).
- [44] S.M. LUZ, J. DEL TIO, G.J.M. ROCHA, A.R. GONCALVES, A.P. DEL'ARCO JR, «Cellulose and cellulignin from sugarcane bagasse reinforced polypropylene composites: Effect of acetylation on mechanical and thermal properties», *Composites Part A: Applied Science and Manufacturing*, 39, 1362-1369, (2008).
- [45] W. QIU, T. ENDO, T. HIROTSU, «Structure and properties of composites of highly crystalline cellulose with polypropylene: Effects of polypropylene molecular weight», *European Polymer Journal*, 42, 1059-1068, (2006).
- [46] W. QIU, F. ZHANG, T. ENDO, T. HIROTSU, «Preparation and Characteristics of Composites of High-Crystalline Cellulose with Polypropylene: Effects of Maleated Polypropylene and Cellulose Content», *Journal of Applied Polymer Science*, 87, 337-345, (2003).
- [47] S.K. NAYAK, S. MOHANTY, S.K. SAMAL, «Influence of short bamboo/glass fiber on the thermal, dynamic mechanical and rheological properties of polypropylene hybrid composites», *Materials Science and Engineering A*, 523, 32-38, (2009).
- [48] F. VILASECA, A. VALADEZ-GONZALEZ, P.J. HERRERA-FRANCO, M. ÀNGELSPÉLACH, J.P. LÓPEZ, P. MUTJÉ, «Biocomposites from abaca strands and polypropylene. Part I: Evaluation of the tensile properties», *Bioresource Technology*, 101, 387-395, (2010).
- [49] Y. LEI, Q. WU, «Wood plastic composites based on microfibrillar blends of high density polyethylene/poly(ethylene terephthalate)», *Bioresource Technology*, 101, 3665–3671, (2010).

# Evaluation of natural biodegradation of low-density polyethylene/modified corn flour composites

Samira SAHI<sup>1\*</sup>; Hocine DJIDJELLI<sup>2</sup>; Amar BOUKERROU<sup>2</sup>

*1: Laboratory of Advanced Polymer Materials, Department of Process Engineering, Faculty of technology, University A. Mira of Bejaia, Bejaia (06000), Algeria.*

\*samira.sahi@univ-bejaia.dz

Received: 12 May 2023; Accepted : 27 July 2023; Published: 29 July 2023

## Abstract

*Composites based of low density polyethylene (LDPE) reinforced with acetylated corn flour (ACF) at proportion of 10, 30 and 50 (%.Wt) were prepared. The biodegradation of resulting composites was studied in the environment using the soil burial test. The biodegradation were evaluated by different analysis techniques and were compared with the results recorded on these composites before the biodegradation test. Differential scanning calorimetry (DSC) analysis showed an increase of the melting enthalpy and crystallinity of LDPE with evidence of degradation. The biodegradability of the composites was enhanced with increasing ACF content in the matrix. This result was supported by decrease in mechanical properties, by weight loss and degraded surface of composites observed through morphological studies.*

**Keywords:** *Low density polyethylene, Corn flour, Properties, Biodegradation.*

## I. Introduction

Synthetic polymers are increasingly present in daily life. However, they are rarely used alone, but combined with other materials, thus allowing the properties of each to be associated.

Also, the properties of a single polymer are insufficient to confer on the object that one wishes to manufacture all the desired properties in terms of rigidity, mechanical resistance, lightness or other physico-chemical, electrical, optical property, which has led to the first research on the development of plastic materials including renewable raw materials of natural origin. Passed to the background as an additional motivation the preservation of the environment and public health.

In fact, with a concern for the preservation of fossil resources, and in an effort to reduce pollution, biodegradable composite materials have been developed alongside traditional composites. These new materials are of additional interest. They are easily degradable and therefore harmless to the environment.

In a mixture or not with others synthetic polymers, raw material of vegetable origin most widely used are starch. It was incorporated in conventional plastics with the aim to give a certain level of biodegradability in the resulting composites and it is an inexpensive, renewable and natural polymer [1]. However, applications of starch materials are limited by poor mechanical strength properties and high moisture [2].

To improve the mechanical properties of materials blending starch with other polymers such as low-density polyethylene (LDPE), chemically modified starches was used, this modification often makes the starch more hydrophobic, which improves the interfacial contact between starch granule and polymer, thereby enhancing stability of resulting materials in water [3]. (Kim, 2003) [4]. Cao et al. [5] found 13% improvement in tensile strength, 14% in flexural strength and 30% in impact respectively for polyester reinforced with bagasse fiber after alkali treatment.

In this study the possibility to prepare LDPE/acetylated corn flour blends instead LDPE/acetylated corn starch was investigated because corn flour is cheaper than corn starch (is obtained with less processing steps and thus less water and energy consumption) [6]. In addition, corn flour is completely biodegradable by microorganisms. It composed of 75–87% starch and 6–8% protein [7].

Several formulations with LDPE and acetylated corn flour (ACF) were prepared and characterized. The study of their biodegradability in a natural environment by burial in soil was developed and compared to those before degradation.

## II. Material and methods

### II.1 Materials

Low density polyethylene (LDPE), BASEL 2420F, was obtained from Flay packaging, Bejaia, Algeria. Corn flour was provided by the AGRO CEREALES/Moulin Royal-Akbou Algeria and it has less than 7 % moisture content and the particle size was 90  $\mu\text{m}$ . Acetic anhydride and sodium hydroxide were obtained from Fluka.

## II.2 Methods

### Acetylation of corn flour

Acetylation was done with the method proposed by Gunaratne and Corke [8]: Corn flour was dissolved in distilled water. The pH was adjusted with 1 M NaOH to 8.0-8.5. Acetic anhydride was added to the blend and then mechanically stirred for 30 min. The blend was washed with distilled water three times and dried at 35 °C.

### Samples preparation

LDPE (F0) and LDPE/ACF composites at ratio of 90:10 (F10), 70:30 (F30) and 50:50 (F50) (wt.%) were prepared using twin-screw extruder (model Micro compounder DSM Explore). The extrusion conditions were as follows: the temperature mixing zone of the barrel was maintained at 150 °C, with a screw speed of 50 rpm and a mixing time of 5 min. After extrusion, the products are injected into a mold at 5 atm and at room temperature. The material was then compacted, and maintained under pressure and the cooled part is ejected. The injection mold used in this machine is only one fingerprint in dumb-bell shape, with the following dimensions: useful length 63 mm, useful width 10 mm and thickness 3 mm.

### Biodegradability test

The biodegradability test was produced by burying samples in the soil. It was carried out as described by Santayanon and Wootthikanokkhan [9] with some modifications. The soil burial was recovered from a landfill. Ten specimens of each formulation were buried at a depth of 10 cm and after 180 days of burial, they were collected. The specimens were weighed before and after burial. In the latter case the specimens were first rinsed with distilled water after removal from the burial site and then dried at 60 °C for 48 h prior to their weighing and analyzed. The specimens of each composition were weighed at precision 0.0001 g.

### Spectroscopy analysis (FTIR)

FTIR spectra were recorded using an infrared spectrophotometer Fourier Transform Model SHIMADZU FTIR. Potassium bromide (KBr) disks were prepared from powdered samples mixed with dry KBr in the ratio of 1:100. The spectra were recorded in a transmittance mode from 4000 to 400  $\text{cm}^{-1}$  at a resolution of 4  $\text{cm}^{-1}$ .

### Morphological studies

SEM analyses were performed using Scanning Electron Microscope (Jeol JSM 6100 Model). The specimens had been coated with thin film of gold/vanadium before observation.

### Differential scanning calorimetry (DSC)

The melting temperatures ( $T_m$ ), the melting enthalpy ( $\Delta H_m$ ) and the degree of crystallinity ( $X_c$ ) of LDPE were determined using a differential scanning calorimeter (DSC) (model Q200, TA Instrument). Two heating cycles were used for each sample. The samples were first heated from -20 to 200 °C at a constant rate of 20 °C/min to eliminate their thermal history, and then cooled to -20 °C and immediately reheated to 200 °C. The second scan was done at the same heating rate. Nitrogen gas was supplied to purge the system at a flow rate of 150 ml/min.  $T_m$  was determined from the second scan, it was taken as the maximum of the endothermic melting peak from the heating scans.  $\Delta H_m$  was obtained from the areas of melting peaks.  $X_c$  was obtained from the ratio between the melting enthalpy of the samples ( $\Delta H_m$ ) and the melting enthalpy of 100% crystalline LDPE (277,1 J/g) (Pedroso, Rosa, 2005).

### Mechanical properties

Measurements of the tensile properties were performed using a Shimadzu tensile testing machine (Model Autograph AGS-X 10kN). Measurements were performed at a 10 mm  $\text{min}^{-1}$  crosshead speed at ambient temperature. The device provides access to the force  $F$  as a function of elongation ( $L-L_0$ ) where  $L_0$  is the initial length of the film. For each formulation, five specimens were tested. The Young's modulus, strain and stress were determined.

### Morphological studies

SEM analyses were performed using Scanning Electron Microscope (Jeol JSM 6100 Model). The specimens had been coated with thin film of gold/vanadium before observation.

## III. Results and discussion

### FTIR analysis

The FTIR spectra of corn flour before and after treatment are shown in Fig. 1. The spectra of corn flour have characteristic profiles to native starch. According to the literature [10, 11], the chemical functions for each absorption band which appears on the FTIR spectra of starch are given as follow:

There are three characteristic bands of starch between 990  $\text{cm}^{-1}$  and 1160  $\text{cm}^{-1}$ , attributed to C-O bond stretching. The bands at around 1150  $\text{cm}^{-1}$ , 1080  $\text{cm}^{-1}$  were characteristic of C-O-H in starch, and the band between 990  $\text{cm}^{-1}$  and 1030  $\text{cm}^{-1}$  was characteristic of the anhydroglucose ring O-C stretch. The band at 1655  $\text{cm}^{-1}$  is attributed to the water adsorbed in the amorphous region of starches. The band at 2920  $\text{cm}^{-1}$  is characteristic of C-H stretch. An extremely broad band due to

hydrogen-bonded hydroxyl groups appeared at  $3400\text{ cm}^{-1}$  which ascribed to the complex vibrational stretches coupled with free, inter and intramolecular bound hydroxyl groups, which made up the gross structure of starch.

The FTIR spectra of native corn flour (NCF) and treated corn flour (TCF) show similar profiles (Fig. 1) except for the band located between  $3700$  and  $3000\text{ cm}^{-1}$ , which is reduced on ACF.

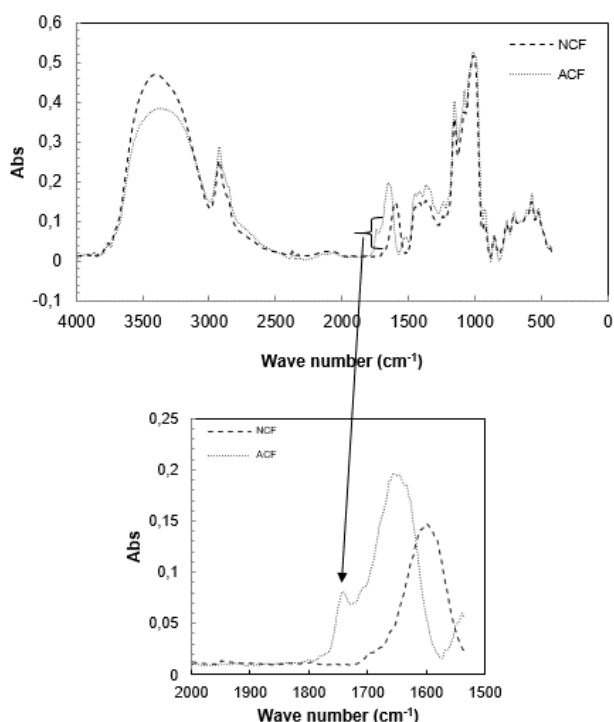
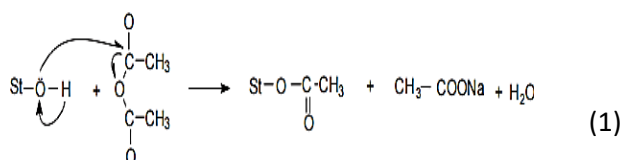


**Figure 1.** FTIR spectra of treated (ACF) and untreated corn flour (NCF)

The reduction in this band is mainly attributed to the decrease in the hydrophilic nature of corn flour after treatment, as following in the reaction (1).

Other relevant peak is that obtained for ACF at  $1745\text{ cm}^{-1}$ , arising from the acetyl group ( $\text{C}=\text{O}$  stretching) in the products [12].



#### Differential scanning calorimetry (DSC) analysis

Fig. 2 shows the DSC curves obtained during second heating of the different formulations before (bf) and after (af) 180 days of burial in soil.

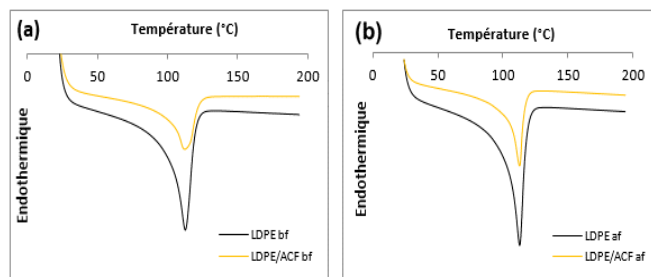


**Figure 2.** DSC curves of LDPE and LDPE/ACF composites: (a) before and (b) after 180 days of burial in soil.

We see that the thermograms recorded one endothermic peak corresponding to the melting temperature of the matrix. The  $T_m$  was taken by the maximum of the endothermic melting peak.

Table 1 shows the average values of the melting temperature ( $T_m$ ), melting enthalpies ( $\Delta H_m$ ) and crystallinity ( $X_c$ ) of all composites before and after 180 days of burial in soil.

**Table 1.** DSC test results of LDPE and LDPE/ACF composites obtained from the second heating curves, before (Bf) and after (Af) 180 days of burial in soil.

Type of formulation		$T_m$ (°C)		$\Delta H_m$ (J/g)		$X_c$ (%)	
		Bf	Af	Bf	Af	Bf	Af
LDPE	F0	112,7	112,8	79,12	97,72	28,55	35,27
LDPE/ACF	F10	112,4	112,1	45,8	76,03	16,53	30,57
	F30	112,5	114,0	38,07	65,85	13,74	23,76
	F50	112,5	112,8	34,13	54,15	12,32	18,82

We can see that the  $T_m$  remained constant for different samples. This temperature corresponds to that of pure LDPE which is  $110\text{ }^\circ\text{C}$  (Pedroso, Rosa, 2005 and Walker et al., 2007).

However, the enthalpy of fusion increased, indicating an increasing in the crystallinity of LDPE, which may reflect biodegradation of the amorphous portion of the matrix by the microorganisms present in the soil. Therefore, microbial degradation leads to an increase in the overall degree of crystallinity of the polyethylene sample. These results are confirmed experimentally by several researchers [13, 14].

#### Tensile properties

Figs. 3 illustrate a comparison in mechanical properties (a) Young's modulus, (b) tensile strength and (c) elongation at break of pure LDPE and those reinforced with ACF for different formulations before and after degradation.

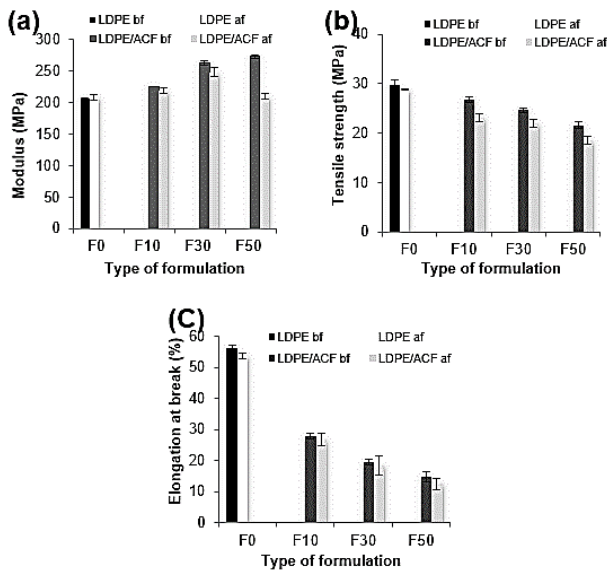


**Figure 3.** Tensile properties of pure LDPE and LDPE/ACF composites before and after 180 days of burial in soil (a) Young's modulus, (b) tensile strength and (c) elongation at break.

After 6 month of burial in th soil, the trend remains the same in all samples and the same behavior was observed for Modulus, tensile strength and elongation at break (i. e. these parameters had a trend to decrease with increasing filler content in the matrix). Comparing these results with those before degradation, the decrease in these properties can be seen clearly in particular for formulations F50 indicating that the samples became weaker after biodegradation. This result indicated that the addition of ACF enhanced the biodegradability of LDPE. It was also observed that the biodegradability of the composites enhanced with increasing ACF content. Shah et al. [15], indicated that the variations in the tensile property are often taken as a direct indication of the biodegradation.

#### Weight loss

Figure 4, shows the weight loss results recorded for pure LDPE and its composites with ACF after 180 days burial in soil. The percentage loss in weight of pure LDPE maintained at 0.12%, but this loss becomes more important with incorporation and the increase of ACF content in the matrix, this due to the presence of corn flour which easily susceptible to the attack of microorganisms [6]. After burial in sol, we recorded 5.65% in decrease of weight for LDPE reinforced with 30 (wt.%) of ACF and it was 7.32% for those blended with 50 (wt.%). Danjaji et al. [16] recorded 2% in decrease of a weight for PE/sago starch 40 (wt.%) composite after 12 months inside a sandy soil containing left-over food. Therefore, we can say that this method is an accelerated method of degradation compared to others.

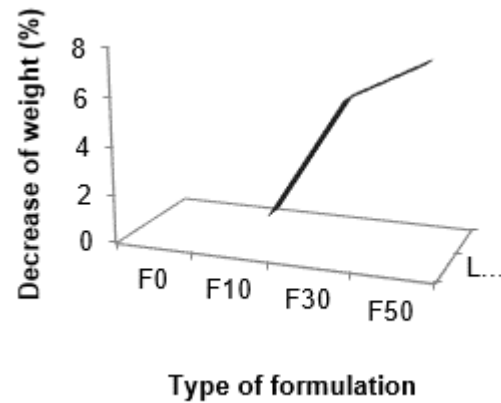


**Figure 4.** Weight loss of pure LDPE and LDPE/ACF after 180 days of burial in soil.

#### Morphological test

SEM micrographs of the pure LDPE and composites with the highest ACF content (F50) before and after 180 days of burial in soil are presented in Fig. 5. The latter shows a smooth surface of pure LDPE. However, LDPE/ACF blends were sensitive to biodegradation. This result was evident by the presence of various holes on the surface. These be a sign of the rate of biodegradation and confirmed the ACF elimination by microorganisms. Corn flour consumption by bacteria caused holes in the polymer matrix and eventually the degradation of LDPE.

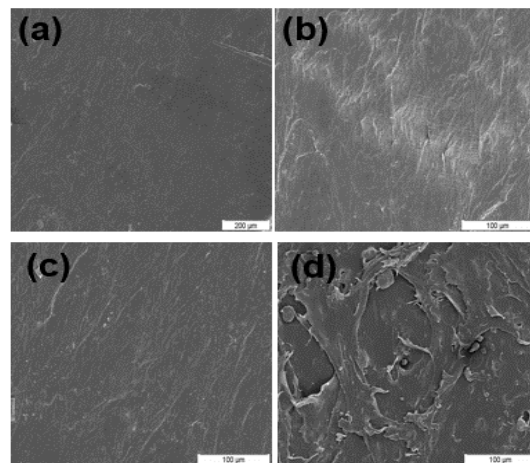


**Figure 5.** SEM micrographs of: pure (a) LDPE before; (b) LDPE after; (c) LDPE/ACF at 50 (wt.%) before; and (d) LDPE/ACF at 50 (wt.%) after 180 days of burial in soil.

#### IV. Conclusions

Study consists on the incorporation of acetylated corn flour in LDPE matrix. Soil burial test was carried to evaluate the biodegradation of resulting composites. As well a comparative study before and after soil burial was made. Degradation study shows that landfills soil burial resulting in weight loss,

presence of the holes in surface and decrease of mechanical properties. LDPE/ACF composites show rapid degradation after 180 days in soil. Therefore, the use of ACS as filler in LDPE is advantageous from both economic and environmental points of view and has potential applications in the development of biodegradable composite materials.

#### **Conflict of interest**

The authors declare that they have no conflict for financial interests or personal relationships that how can influence the work reported in this paper.

#### **References**

- [1] Y. S. Lu, L. Tighzerta, P. Dole, D. Erre. Preparation and properties of starch thermoplastics modified with waterborne polyurethane from renewable resources. *Polymer* 23, 9863-9870, 2005.
- [2] L. Avérous. Biodegradable multiphase systems based on plasticized starch. *Journal of macromolecular Science. Part C: Polymer Review* 44, 231-274, 2004.
- [3] M. Kim. Evaluation of degradability of hydroxypropylated potato starch/polyethylene blend films. *Carbohydrate Polymer* 54, 173-181, 2003.
- [4] D. Ray, B. K. Sarkar, N. R. Rose. Impact fatigue behavior of vinyl ester matrix composites reinforced with alkali treated jute fibres. *Composites: Part A* 33, 233-241, 2001.
- [5] Y. Cao, S. Shibata, I. Fukumoto. Mechanical properties of biodegradable composites reinforced with bagasse fibre before and after alkali treatments. *Composites: Part A* 37, 423-429, 2006.
- [6] F. Jbilou, S. Galland, F. Ayadi, L. Belard, P. Dole, V. Desjardin, R. Bayard, P. Degraeve. Biodegradation of corn flour-based materials assessed by enzymatic, aerobic, and anaerobic tests: Influence of specific surface area. *Polymer Testing* 30, 131-142, 2010.
- [7] F. Jbilou, C. Joly, S. Galland, L. Belard, V. Desjardin, R. Bayard, P. Dole, P. Degraeve. Biodegradation study of plasticised corn flour/poly(butylene succinate-co-butylene adipate) blends. *Polymer Testing* 32, 1565-1575, 2013.
- [8] A. Gunaratne, H. Corke. Influence of prior acid treatment on acetylation of wheat, potato and maize starches. *Food Chemistry* 105, 917-925, 2007.
- [9] R. Santayanon, J. Wootthikanokkhan. Modification of cassava starch by using propionic anhydride and properties of the starch-blended polyester polyurethane *Carbohydrate Polymer* 51, 17-24, 2003.
- [10] J. Xin, Y. Wang, T. Liu. Influence of Pretreatment on Cold Water Solubility and Esterification Activity of Starch. *Advanced Journal of Food Science and Technology* 4, 270-276, 2012.
- [11] A. C. V. Solano, C. R. Gante. Development of biodegradable films based on blue corn flour with potential applications in food packaging. Effects of plasticizers on mechanical, thermal, and microstructural properties of flour films. *Journal of Cereal Science* 60, 60-66, 2014.
- [12] H., Muljana, F. Picchioni, Z. Knez, H. J. Heeres, L. P. B. M. Janssen. Synthesis of fatty acid starch esters in supercritical carbon dioxide. *Carbohydrate Polymer* 82, 346-354, 2010.
- [13] W. Shujun, Y. Jiugao, Y. Jinglin. Preparation and Characterization of Compatible and Degradable Thermoplastic Starch/Polyethylene Film. *Polymer Degradation Stability* 87, 395-401, 2005.
- [14] F. C. Chiu, S. M. Lai, K.T. Ti. Thermoplastic cassava starch/sorbitol-modified ontmorillonite nanocomposites blended with low density polyethylene : properties and biodegradability study. *Polymer Testing* 28, 243-250, 2009.
- [15] A. A. Shah, F. Hasan, A. Hameed, S. Ahmed. Biological degradation of plastics : A. *Biotechnology Advances* 26, 246-265, 2008.
- [16] D. Danjaji, R. Nawang, U. S. Ishiaku, H. Ismail, Z. A. M. Ishak, *Polymer Testing* 21, 75-81, 2002.

# Study of PHBV/PP mixtures: Preparation and physicochemical characterization

Noura HAMOUR <sup>1\*</sup>, Nadira BELLILI <sup>1</sup>, Badrina DAIRI<sup>1</sup>, Amar BOUKERROU <sup>1</sup>, Johnny BEAUGRAND <sup>2,3</sup>

<sup>1</sup>Laboratoire des Matériaux Polymères Avancés (LMPA), Faculté de Technologie, Université de Bejaia, 06000 Bejaia, Algeria

<sup>2</sup>INRA, URCA, UMR614 Fractionnement des AgroRessources et Environnement, 51100 Reims, France

<sup>3</sup>INRA, UR1268 Biopolymères Interactions Assemblages, 44300 Nantes, France \*Corresponding author email:

[noura.hamour@univ-bejaia.dz](mailto:noura.hamour@univ-bejaia.dz)

Received 2 May 2023; Accepted: 27 July 2023; Published: 29 July 2023

## Abstract

*This research work consists in studying the structure-properties relationships of biopolymer mixtures based on poly(3-hydroxybutyrate-co-3-hydroxyvalerate) (PHBV) and polypropylene (PP) elaborated by casting process according to the composition in terms of morphology, structure and thermal properties. The results showed a synergistic effect of glycerol addition on the thermal and morphological properties of the PHBV/PP blends.*

**Keywords:** Blend, Miscibility, Polymer, Plasticization.

## I. Introduction

Man has always used natural polymers (cotton, wool, hemp...) after as materials [1, 2]. However, since the discovery of polymerization and the production of synthetic polymers, they have become an essential part of our daily lives and it is now difficult to do without them. In a century the production of plastics has grown exponentially, this increased consumption has generated several problems: the rarefaction of the fossil resource because they are non-renewable and the pollution of the environment.

This is why materials from renewable resources are receiving increasing interest from the academic and industrial world. They are very varied in nature and often present interesting characteristics. However, some important properties of biobased polymers do not yet rival those of conventional petrochemical polymers such as polyethylene and polypropylene [3,4]. To be able to replace in the future a significant part of the polymers of fossil origin by biosourced polymers, multiple challenges are to be met. A great deal of research has been conducted over the past decade to develop more efficient materials from renewable resources, but there is still a long way to go before they can find their place in the competitive polymer market.

Among the class of biodegradable polymers derived from renewable resources, polyesters are undoubtedly those with the most promising future to replace polyolefin. Among them,

we can mention poly(hydroxyalkanoate) (PHA) or poly(lactic acid) (PLA) [5,6] which is produced on an industrial scale by companies such as Nature Works (USA) or PURAC Biomaterials (Holland). Poly (3-hydroxybutyrate-co-3-hydroxyvalerate) or PHBV [7], produced by a wide variety of bacteria that store them as an intracellular energy reserve [8]. PHBV also has thermal and mechanical properties comparable to conventional thermoplastics such as polypropylene (PP). However, their cost is still too high and some of their properties are still too weak to replace petroleum-based polymers.

Polymer blending is an approach that allows the development of new materials with desired properties. Making these blends from existing polymers is less expensive than developing a new polymer. Moreover, the processes are generally quite simple (extrusion, internal mixer, injection...). Polymer blends are interesting because their properties depend on the parent polymers, properties that can therefore be varied with the blend composition [9, 10].

It is in this context that the subject of this work was born, the study of PHBV/PP mixtures prepared by solvent way (casting) on a whole range of composition and the highlighting of the various structure-properties relations. Morphological and structural characterization and thermal properties of mixtures will be addressed.

## II. Material and methods

### II.1. Materials

Poly(3-hydroxybutyrate-co-3-hydroxyvalerate) PHBV was supplied by Natureplast under the trade name PHI002 with a melt flow index (MFI) of g/10 min (190 °C/2.16 kg) (ISO 1133) and a melting temperature of 170–176 °C (values from supplier datasheets). Isotactic polypropylene (PP500P ©) used in this study as matrix was provided by SABIC (Saudi Arabia) with a melt flow index (MFI) of 3 g/10 min (230°C/2.16 kg) (ASTMD-1238) and a density of 0.9 g/cm<sup>3</sup> (values from supplier datasheets). Glycerol (M, 92.09g/mol, density, 1.26 g/cm<sup>3</sup>), chloroform (M, 119.38g/mol, density, 1.47 g/cm<sup>3</sup>), and xylene (M, 106.17, density, 0.86 g/cm<sup>3</sup>), which are provided by Sigma-Aldrich (St. Louis, USA).

### II.2. Composites processing

Different formulations of PHBV/PP were prepared by casting solution. The formulation contain PHBV is mixed in chloroform which is a good solvent for PHBV and the PP formulation is mixed in xylene. These two solutions are placed in a mechanical shaker for three hours at 62°C for PHBV and two hours at 140 °C for a PP. After mixing the two solutions PHBV and PP at room temperature for 10 minutes under stirring adds to this 1 ml of glycerol. The solutions without and with plasticizer, is deposited on petri dishes so that the solvent is evaporated. The films should be left in the open air for three days before placing in the oven at a temperature of 40°C for 24 hours.

The different formulations used are summarized in the Table 1.

**Table 1.** Samples used in this study

Formulations	PHBV/PP (%)	PHBV (g)	PP (g)	Xylene (ml)	Chloroform (ml)
PHBV <sub>100</sub>	-	1	-	-	100
PP <sub>100</sub>	-	-	1	100	-
PHBV <sub>80</sub> PP <sub>20</sub>	80/20	0.8	0.2	20	80
PHBV <sub>70</sub> /PP <sub>30</sub>	70/30	0.7	0.3	30	70
PHBV <sub>60</sub> /PP <sub>40</sub>	60/40	0.6	0.4	40	60
PHBV <sub>50</sub> /PP <sub>50</sub>	50/50	0.5	0.5	60	40

### II.3. Techniques

#### 2.3.1. Microstructural analysis

Shimadzu FTIR 8400S model in the range of 4000–500 cm<sup>-1</sup> measured fourier transform infrared (FTIR) spectra. The equipment was operated in absorbance mode with four scans at a resolution of 4 cm<sup>-1</sup>. Thin films of different samples, which were between 60 and 80 lm in thickness, were prepared by compression moulding at 180 °C for 2 min.

#### 2.3.2. Scanning electron microscopy

Scanning electron microscopy (SEM) was used to monitor the fracture surface of the composites after the samples were frozen in liquid nitrogen. The SEM analysis was performed using an FEI CONTA 200 system.

#### 2.3.3. Thermogravimetric analysis (TGA)

TGA experiments were carried out on a Setaram TG-DTA 92–10 thermal analyzer, using a scanning rate of 10 °C min<sup>-1</sup> under nitrogen in the temperature range starting from 25 °C to 700 °C.

#### 2.3.4. Differential scanning calorimetric analysis (DSC)

The DSC measurements were conducted using a DSC-LINSEIS differential scanning calorimeter with nitrogen as the purge gas. Samples of approximately 5–10 mg were analysed in the temperature range of 25–200 °C with a heating rate of 20 °C.

The crystallinity index of PHBV, PP and PHBV/PP mixtures can be determined from the following equations:

$$\chi_c(\%) = \frac{\Delta H_m}{\Delta H_m^0} \times \frac{100}{\phi}$$

Where,  $\phi$  is the mass fraction of the dispersed phase in the mixtures, is the enthalpy of fusion (J/g) calculated from the peak of fusion in the DSC curve and is the heat of fusion for fully crystalline PHBV (146.6 J/g) [11], and for fully crystalline PP (209 J/g) [12].

## III. Results and discussion

### III.1. Evolution of the chemical structure by IRTF spectroscopy

Changes in chemical structure in PP/PHBV mixtures were evaluated by FTIR spectroscopy (Figure 1). From the spectra of virgin PHBV (Figure 1 (a)) we observe a band at 2946 cm<sup>-1</sup> attributed respectively to the asymmetric and symmetric elongation of C-H in the CH<sub>3</sub> methyl group, the deformation and symmetry of the CH<sub>3</sub> group causes an absorption for respective wave numbers of 1453 and 1379 and 1303 cm<sup>-1</sup>. An intense and neat band at 1725 cm<sup>-1</sup> is attributed to the elongation of the C=O carbonyl groups of the crystalline parts in PHBV [13]. The C-O-C elongation absorption bands are located between 800, 1000 cm<sup>-1</sup>, and the band at 1218 cm<sup>-1</sup> is assigned to the vibration of the methylene (CH<sub>2</sub>) group [14].

Concerning the spectrum of pure PP (Figure 1 (a)) reveals also the presence of several absorption bands we cite :

A large band with a peak centered at 2938 cm<sup>-1</sup> attributed to the asymmetric elongation vibration of the CH<sub>3</sub> group.

A very large band with peaks at 2925 and 2784 cm<sup>-1</sup> corresponding to the asymmetric elongation vibrations of CH<sub>2</sub>, CH<sub>3</sub> groups. A series of peaks between 1502 and 1342 cm<sup>-1</sup>

corresponding to the symmetric deformation of CH<sub>3</sub> group and shear deformation of CH<sub>2</sub> group. A series of peaks between 1200 and 1000 cm<sup>-1</sup> characteristic of elongation deformations of C-C and C-H bonds [15].

On the spectra of PP/PHBV mixtures at different compositions (Figure 1 (b)) show the characteristic bands of both homopolymers (PP and PHBV) without any change which indicates the absence of any interaction between these two materials [16,17].

The spectra of the PP/PHBV mixtures plasticized with glycerol (Figure 1 (c)) reveal bands positioned at 990, 910 and 844 cm<sup>-1</sup> attributed to the absorbance of the epoxy group, a band relative to the C=O group at 1734 cm<sup>-1</sup> but the intensity of the bands increases steadily, in addition to the bands characteristic of polypropylene.

Several changes were observed in the spectra of the plasticized mixtures, the most important being:

- The appearance of a new band in the 3261 cm<sup>-1</sup> region which can be attributed to bound hydroxyl groups (-OH). This intensity is more pronounced for the PHBV<sub>60</sub> /PP<sub>40</sub> formulation.

- Increase of the intensity of the 1724 cm<sup>-1</sup> band of the carbonyl group (C=O) of the PHBV<sub>60</sub> /PP<sub>40</sub> formulation.

All these changes confirm the existence of interaction between the functions of the groups of the PP/PHBV mixture and the plasticizer (glycerol).

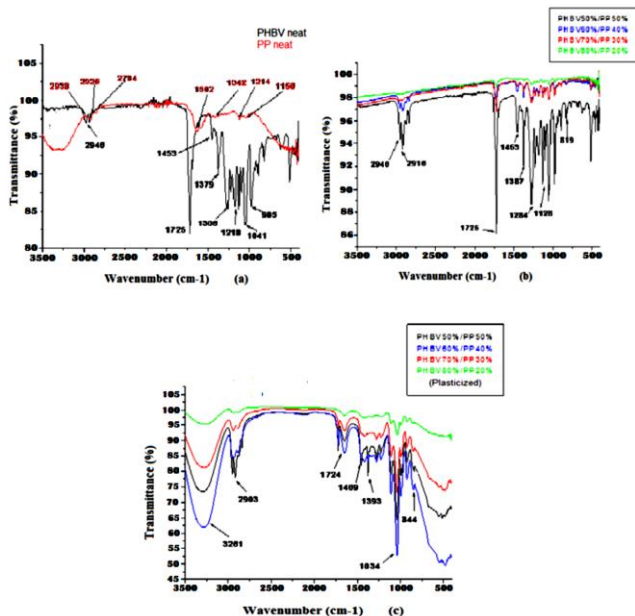


Figure 1. FTIR spectra of the Virgin PHBV, PP (a), PHBV/PP (b) before plasticized and PHBV/PP (c) after plasticized.

### III.2 Microscopic observations

SEM is used to characterize the dispersion state of PP in the PHBV matrix and evaluate the degree of miscibility between the two polymers (Figure 2).

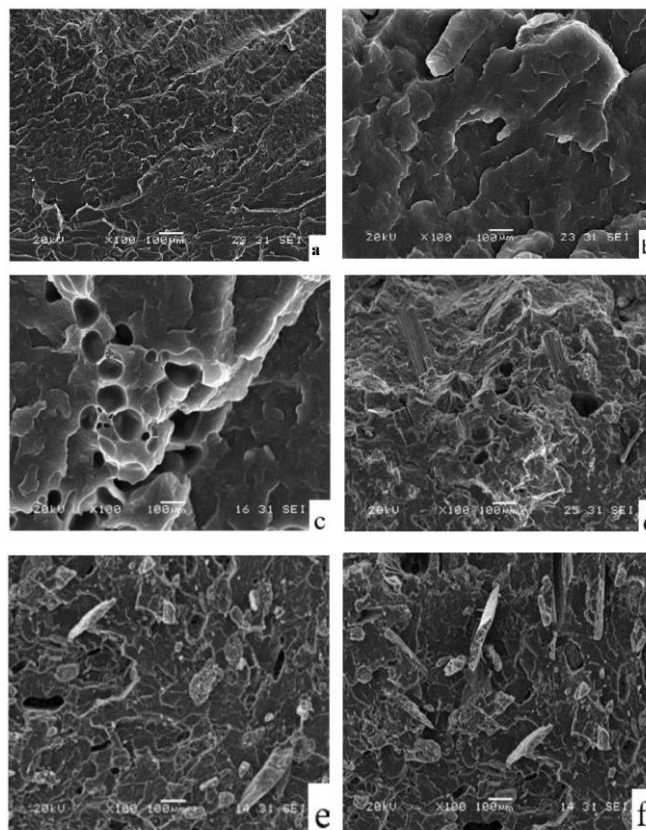


Figure 2. SEM Micrographs of fractured surfaces (a, b, c, d, e and f) for formulations: (a) virgin PHBV, (b) virgin PP, (c) PHBV 80/20, (d) PP/PHBV 70/30, (e) PP/PHBV 60/40 and (f) PP/PHBV 50/50 before plasticized.

The micrographs of PHBV (Figure 2 (a)) and PP (Figure 2 (b)) show an irregular and rough fracture surface due to its crystal structure. The PHBV image shows white trace over the entire surface which is attributed to the presence of organic fillers in the commercial PHBV [18].

Figure 2 (c, d, e et f) shows the scanning electron microscopy images of the fractured surfaces of the different PP/PHBV blends. The micrographs in figure 2.(c et d) (20% et 30% by weight of PP) show spherical domains of the minor phase dispersed in the continuous phase (matrix) and the presence of void at the interface between the two phases. Moreover, the surfaces of the particles extracted from the matrix are smooth and without any visible roughness. All these characteristics are typical of immiscible mixtures. Similar images were obtained by Hoseini and al [19], Kim and al [9] for 75/25 LDPE/PLA blends, and 80/20 and 20/80 LLDPE/PLA blends. Such images have also been observed for many binary mixtures such as PE/PP [20], PE/PS [21], PE/collagen [22]. In general, a roughness of the particle surface is evidence of good interfacial adhesion between the particles and the matrix [22-24].

Micrographs of the 50/50 and 40/60 PP/PHBV blends (Figures 2.e-f) reveal co-continuous morphologies that result from coalescence of domains of the same phase. At these compositions, it becomes difficult to distinguish the dispersed phase from the matrix [10].

These morphologies consist of only two large polymer domains, in this case PP and PHBV, extending completely over the entire structure. However, it is also observed, in the co-continuous structure, that each continuous phase encompasses micro-domains of the other phase, i.e., sub-inclusions of the PP are present inside the PHBV and vice versa. The formation of these under-inclusions can be explained by the fact that, at phase inversion, a small amount of each phase is surrounded by the growing continuous phase [25].

Regarding the effect of glycerol addition on the morphology of PP/PHBV blends, the comparison of different micrographs show drastic changes in the morphology of the materials (Figures 3). With the incorporation of 1% of glycerol in PP/PHBV 80/20 and PP/PHBV 70/30, the size of the PP nodules is considerably reduced and the dispersed phase becomes more deformed and less discernible, as can be seen clearly in Figure 3(a e b). This effect is even more pronounced in PP/PHBV 60/40 (Figure 3 (c)) and 50/50 (Figure 3 (d)) mixtures, which reveals an almost homogeneous morphology at this magnification suggesting an improvement of the miscibility between the two mixture components.

It can be inferred that the addition of glycerol acted synergistically to produce smaller nodules and a relatively uniform distribution of them within the PHBV matrix.

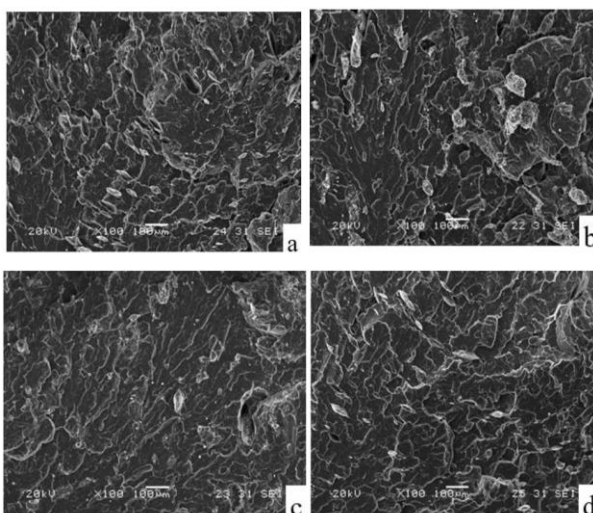


**Figure 3.** SEM Mmicrographs of fractured surfaces (a, b, c and d) after plasticized for formulations: (a) PP/PHBV 80/20, (b) PP/PHBV 70/30, (c) PP/PHBV 60/40 and (d) PP/PHBV 50/50.

### III.3. Thermogravimetric analysis (TGA)

Thermal stability is defined as the maximum temperature the material can withstand without irreversible mass loss. The thermogravimetric analysis allows to follow the variation of the mass of a sample according to the temperature and thus to reach the parameters of decomposition of a material. To facilitate reading, it is convenient to represent the derived curve (DTG) of the TGA. This curve makes it easier to identify mass loss phenomena since they appear as peaks. Figures 4 and 5 illustrate, respectively, the thermal decomposition curves (TG) and the curves of their first-order derivatives (DTG) for PP, PHBV and their mixture, the most important characteristic temperatures of the different materials are summarized in Table 2.

**Table 2.** TGA data for neat PHBV, PP and PHBV/PP blend

Formulations	Td (°C)	T <sub>50%</sub> (°C)	Tmax (°C)	Vmax (%/mn)	Residue rate (%)
PP <sub>100</sub>	421	434	440	3.41	0.85
PHBV <sub>100</sub>	262	272	280	1.17	1.35
PHBV <sub>60</sub> /PP <sub>40</sub>	185	270	270	3.2	1.25
PHBV <sub>50</sub> /PP <sub>50</sub>	200	285	272	2.8	0.96
PHBV <sub>60</sub> /PP <sub>40</sub> (plasticized)	240	250	255	1.9	0
PHBV <sub>50</sub> /PP <sub>50</sub> (plasticized)	240	260	268	1.65	0

In Figure 4(a) the loss of mass of PP and PHBV took place in a single regular step, to wait towards the end of very low masses which are of the order of 0.85 for PP and 1.35 for PHBV. These results are confirmed in figure 4(b) by the presence of a single peak in the corresponding DTG curve, these results are in agreement with that found in literature [26, 27].

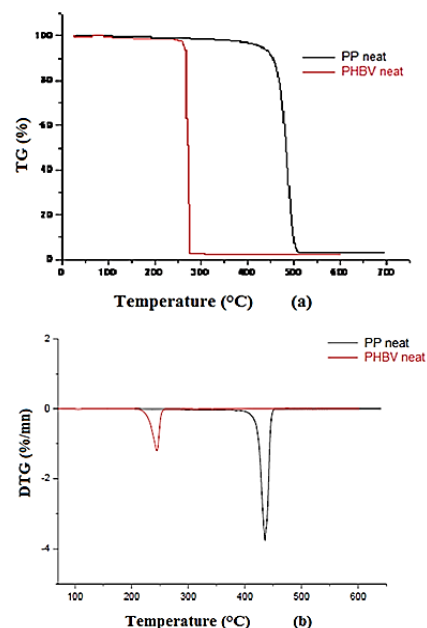


**Figure 4.** Thermal degradation behavior of the neat PHBV and P : (a) TGA thermograms and (b) DTG thermograms.

Examining the results in Table 2, it can be noticed that PP shows more stability than PHBV where the difference between the corresponding temperatures at the onset of their degradation is about 80°C for PP ( $T_d = 421^\circ\text{C}$ ) and ( $T_d = 262^\circ\text{C}$ ) for PHBV. On the other hand, the decomposition of PP took place over a larger temperature range than that of PHBV, which indicates that the decomposition reaction of PHBV is more rapid than PP. Thus, thermal degradation of PHBV results in a greater loss of mass (96%) than PP (98%).

According to the literature [28-30], the thermal degradation of PP occurs by random chain cleavage and follows a radical mechanism. The main pyrolysis products are homologous series of alkenes, alkanes and dines [30]. However, the degradation of PHBV is more complex. Its degradation at temperatures above 200°C includes intermolecular transesterification reactions, which lead to the formation of cyclic and acrylic oligomers, as well as fragmentation, which leads to acetaldehyde and carbon dioxide.

Concerning PHBV/PP mixtures, thermogravimetric curves (Figure 5) show for all compositions, a degradation process in two steps, confirmed by DTG curves (Figure 5(b)) by the presence of two distinct peaks.

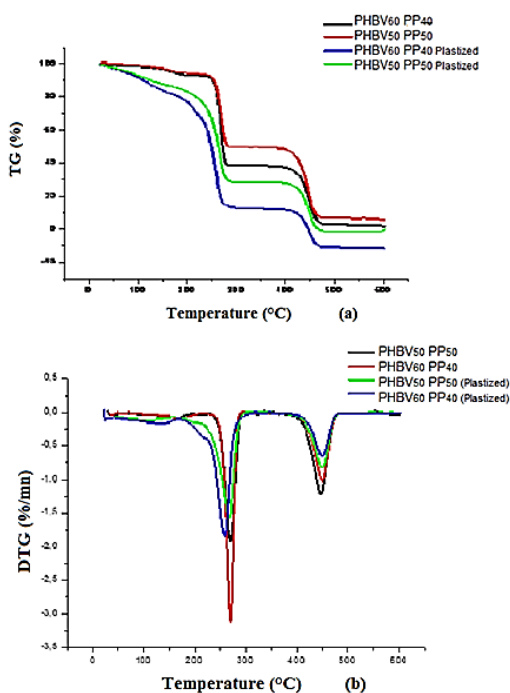


Figure 5. Thermal degradation behavior of the PHBV/PP blend before and after Plasticized: (a) TGA thermograms and (b) DTG thermograms.

The temperature of the first decomposition peak is close to the pure PHBV peak while the second peak is close to that of pure PP. Thus, the initial mass loss of the PHBV/PP mixture is

mainly due to the decomposition of PHBV while the second thermal degradation step is due to the decomposition of PP. Such findings were made during the thermal degradation of the studied mixtures by [31, 32], these authors suggest that the thermal degradation of each component of the studied mixtures occurs independently i.e. it is not affected by the presence of the other component. The negligible amounts of residual masses at 600 °C obtained after the second stage of decomposition, indicates a complete material degradation, although the residue beyond 600°C increases with the increase of the PHBV content.

The TGA and DTG curves of the plasticized formulations presented in figure 5 (a, b), we clearly observe that the thermal degradation profiles follow the same trend (two mass losses). According to the results of Table 2 we notice that the addition of plasticizer to the mixtures PHBV<sub>60</sub>/PP<sub>40</sub> and PHBV<sub>50</sub>/PP<sub>50</sub> leads to a decrease of the temperature of onset of degradation ( $T_d$ ), and this decrease increases with the increase of the quantity of PHBV. This is due to the flexibility of plasticized PHBV/PP blends which have a much lower decomposition temperature than non-plasticized PHBV/PP blends.

#### III.4. Differential scanning calorimetric analysis (DSC)

DSC was used to study the miscibility and possible interactions between PHBV and PP in the mixtures. The values of melting temperatures ( $T_m$ ) and crystallinity rate reported in Table 3.

It can be seen from the results in Table 3 that the values of the melting temperatures ( $T_m$ ) remain relatively unchanged regardless of the proportion of PP in the mixture.

Table 3. Results of melt temperature and crystallinity obtained by DSC

Formulations	Before plasticization		After plasticization	
	$T_r$ (°C)	X (%)	$T_r$ (°C)	X (%)
PP <sub>100%</sub> /PHBV <sub>0%</sub>	169.12	36.8	168.33	31.40
PP <sub>0%</sub> /PHBV <sub>100%</sub>	171.10	/	170.14	/
PP <sub>20%</sub> /PHBV <sub>80%</sub>	170.17	30.2	169.12	27.12
PP <sub>10%</sub> /PHBV <sub>70%</sub>	168.3	25.32	168.10	20.32
PP <sub>50%</sub> /PHBV <sub>50%</sub>	168.8	19.11	167.22	15.33

Concerning the values of the crystallinity rate of each polymer decreases with the addition of the other polymer. This decrease can be attributed to the crystallization of PHBV is limited by the presence of PP; similar results have also been reported on the crystallization behavior of other PHBV-based blends [33, 34]. The effect of the addition of glycerol on the crystallinity of the two polymers in the blend, the results presented on Table 3. It is observed that the percentage of crystallinity tends to

decrease for both polymers. This may be due to the fact that glycerol has a significant influence on the flexibility of the PHBV/PP blend chains and on the intermolecular interactions, probably explained by a certain affinity between the two polymers [35].

#### IV. Conclusions

Mixtures based on PHBV and PP with and without plasticizer (glycerol), were prepared by casting solution.

The morphological study of the different samples, compared to PHBV alone and PP alone, showed that the PHBV/PP mixtures form a biphasic system over the entire compositional range.

The immiscibility between the two components of the mixtures was revealed using SEM analysis, which clearly showed the appearance of a co-continuous morphology for the PHBV<sub>50</sub>/PP<sub>50</sub> mixture while the other compositions of 80/20, 70/30 mixtures led to a dispersed morphology. The dispersion of the PP was significantly refined with the incorporation of the plasticizer (glycerol), due to increased interactions between the components.

Infrared spectroscopy (FTIR) of the unplasticized PHBV/PP mixtures showed the absence of any reaction in these mixtures while the spectra of the plasticized PHBV/PP mixtures showed the existence of interaction between the different constituents. Such interaction preventing reactions between the functional groups of the plasticizer.

Thermal properties (DSC) show that each of the two constituents (PHBV and PP) influences the crystallization of the other in the mixtures. The thermogravimetric analysis showed that the addition of plasticizer to the PHBV<sub>60</sub>/PP<sub>40</sub> and PHBV<sub>50</sub>/PP<sub>50</sub> mixtures leads to a decrease of the temperature of onset of degradation (Td), this decrease increases with the increase of the PHBV quantity.

#### References

1. K. Wang, C. Fu, R. Wang, G. Tao, Z. Xia, High-resilience cotton base yarn for anti-wrinkle and durable heat-insulation fabric, *Compos. Part B*. 212, 108663 (2021).
2. A. Elkhaoulani, F. Z. Arrakhiz, K. Benmoussa, R. Bouhfid, A. Qaiss, Mechanical and thermal properties of polymer composite based on natural fibers: Moroccan hemp fibers/polypropylene, *Mater. Design*. 49, 203–208. (2013).
3. N. Hamour, A. Boukerrou, H. Djidjelli, R. Yefsah, S. Corn, R. El Hage, A. Bergeret, Effect of gamma irradiation aging on mechanical and thermal properties of alfa fiber reinforced

polypropylene composites: Role of alfa fiber surface treatments, *J. Thermoplast. Compos.* **31**, 598- 615 (2018).

4. C. Ihemouchen, H. Djidjelli, A. Boukerrou, F. Fenouillot, Effect of compatibilizing agents on the mechanical properties of high-density polyethylene/olive husk flour composites, *J. Appl. Polym. Sci.* 128, 2224–2229 (2013).

5. N. Hamour, A. Boukerrou, H. Djidjelli, J. Beaugrand, In situ grafting effect of a coupling agent on different properties of a poly(3- hydroxybutyrate-co-3-hydroxyvalerate)/ olive husk flour composite, *Polym. Bull.* **76**, 6275–6290 (2019).

6. B. Bax, J. Müssig, Impact and tensile properties of PLA/Cordenka and PLA/flax composites, *Compos. Sci .Technol.* 68, 1601–1607 (2008).

7. N. Hamour, A. Boukerrou, J. Beaugrand, Influence of hydrothermal ageing of PHBV/olive husk flour composite in acid medium, *Mater. Today: Proc.* **36**, 54–60 (2021).

8. A.M, Gumel, M.S.M, Annuar, Y. Chisti, Recent Advances in the production, recovery and applications of polyhydroxyalkanoates, *J. Polym. Environ.* **21**, 580–605 (2013).

9. Y. F. Kim, C.N. Choi, Y. D. Kim, K. Y. Lee. M. S. Lee, Compatibilization of immiscible poly(*l*-lactide) and low density polyethylene blends *Fibers. Polym.* **5**, 270–274 (2004).

10. J. Li, B. D. Favis, Characterizing co-continuous high density polyethylene/polystyrene blends, *Polym.* **42**, 5047-5053 (2001).

11. L.T. Lim, R. Auras, M. Rubino, Processing technology for poly (lactic acid), *Prog. Polym. Sci.* **33**, 820–852 (2008).

12. A. Rivaton, D. Lalande, J.L. Gardette, Influence of the structure on the  $\gamma$ -irradiation of polypropylene and on the post-irradiation effects, *Nucl. Instrum. Meth B.* 222, 200-187 (2004).

13. I. Zembouai, M. Kaci, S. Bruzard, A. Benhamida, Y.M. Corre, Y. Grohens, A study of morphological, thermal, rheological and barrier properties of Poly(3-hydroxybutyrate-Co-3- Hydroxyvalerate)/polylactide blends prepared by melt mixing, *Polym.. Test.* **32**, 842-851 (2013).

14. Y.X. Weng, X. L. Wang, YZ. Wang, Biodegradation behavior of PHAs with different chemical structures under controlled composting conditions, *Polym. Test.* 30, 372-380 (2011).

15. D. Roy, S. Massey, A. Adnot, A. Rjeb, Action of water in the degradation of low-density polyethylene studied by X-ray photoelectron spectroscopy, *Express. Polym. Lett.* **1**, 506–511 (2007).

16. YX. Weng, Y. Wang, XL. Wang, YZ. Wang, Biodegradation behavior of PHBV films in a pilot-scale composting condition, *Polym.Test.* **29**, 579-587 (2010).

17. Y. Deng, G. N. White, J. B. Dixon, Effect of structural stress on the intercalation rate of kaolinite, *J. Colloid. Interface. Sci.* 250, 379-393 (2002).

18. Z. Qiu, T. Ikehara, T. Nishi, Miscibility and crystallization behaviour of biodegradable blends of two aliphatic polyesters. Poly(3-hydroxybutyrate-co-hydroxyvalerate) and poly(butylene succinate) blends, *Polym.* **44**, 7519–7527 (2003).
19. M. Hoseini, A. Haghtalab, N. Famili, Influence of compounding methods on rheology and morphology of linear low density polyethylene/poly lactic acid, *Appl. Rheol.* **26**, 64746 (2016).
20. S. Jose, A.S. Aprem, B. Francis, M. C. Chandy, P. Werner, V. Alstaedt, S. Thomas, Phase morphology, crystallisation behaviour and mechanical properties of isotactic polypropylene/high density polyethylene blends, *Eur. Polym. J.* **40**, 2105-2115 (2004).
21. B. Chen, X. Li, S. Xu, T. Tang, B. Zhou, B. Huang, Morphology and properties of SEBS block copolymer compatibilized PS/HDPE blends, *Polym.* **43**, 953-961 (2002).
22. M. C. Dascălu, C. Vasile, C. Silvestre, M. Pascu, On the compatibility of low density polyethylene/hydrolyzed collagen blends. II: New compatibilizers, *Eur. Polym. J.* **41**, 1391-1402 (2005).
23. T.S. Omonov, C. Harrats, G. Groeninckx, Co-continuous and encapsulated three phase morphologies in uncompatibilized and reactively compatibilized polyamide 6/polypropylene/polystyrene ternary blends using two reactive precursors, *Polym.* **46**, 12322-12336 (2005).
24. D. Pasquini, E. D. M. Teixeira, A. A. D. S. Curvelo. M.N. Belgacem, A. Dufresne, Surface esterification of cellulose fibres: Processing and characterisation of low-density polyethylene/cellulose fibres composites, *Compos. Sci. Technol.* **68**, 193-201 (2008).
25. R. Su, J. Su, K. Wang, C. Yang, Q. Zhang, Q. Fu, Shearinduced change of phase morphology and tensile property in injection-molded bars of high-density polyethylene/polyoxymethylene blends, *Eur. Polym. J.* **45**, 747-756 (2009).
26. M. Deroiné, A. Duigou, Y. Corre, P. Gac, P. Davies, G. César, S. Bruzard, Seawater accelerated ageing of poly(3-hydroxybutyrate-co-3-hydroxyvalerate), *Polym. Degrad. Stab.* **105**, 237–247 (2014).
27. A. Boukerrou, S. Krim, H. Djidjelli, C. Ihamouchen, J. Martinez. Juan, Study and characterization of composites materials based on polypropylene loaded with olive husk flour, *J. Appl. Polym. Sci.* **122**, 1382–1394 (2011).
28. X. Li, Zhang, J. Li, L. Su, J. Zou, S. Komarneni, Y. Wang, Improving the aromatic production in catalytic fast pyrolysis of cellulose by co-feeding low-density polyethylene, *Appl. Catal. A-Gen.* **455**, 114-121 (2013).
29. R. Zong, Z. Wang, N. Liu, Y. Hu, G. Liao, Thermal degradation kinetics of polyethylene and silane-crosslinked polyethylene, *J. Appl. Polym. Sci.*, **98**, 1172-1179 (2005).
30. J. Borah, T. Chaki, Effect of Organo-Montmorillonite Addition on the Dynamic and Capillary Rheology of LLDPE/EMA Blends, *Appl. Clay. Sci.* **59**, 42-49 (2012).
31. M. Omura, Y. Shirai, H. Nishida, T. Endo, Thermal Degradation Behavior of Poly(Lactic Acid) in a Blend with Polyethylene, *Ind. Eng. Chem. Res.* **45**, 2949-2953 (2006).
32. A. Grisa, M. Zeni, Biodegradation of the flexible PVC in landfills, *Macromol. Symp.* 245-246, 607-610 (2006).
33. Z. Qiu, T. Ikehara, T. Nishi, Miscibility and crystallization behaviour of biodegradable blends of two aliphatic polyesters. Poly(3-hydroxybutyrate-co-hydroxyvalerate) and poly(butylene succinate) blends, *Polym.* **44**, 7519-7527 (2003).
34. Y.S. Chun, W.N. Kim, Thermal properties of poly(hydroxybutyrate-co-hydroxyvalerate) and poly( $\epsilon$   $\epsilon$  - caprolactone) blends, *Polym.* **41**, 2305-2308 (2000).
35. S. Djellali, N. Haddaoui, T. Sadoun, A. Bergeret, Y. Grohens, Structural, morphological and mechanical characteristics of polyethylene, poly (lactic acid) and poly (ethyleneco-glycidyl methacrylate) blends, *Iran. Polym. J.* **22**, 245–275 (2013).

## The effect of a dispersing agent on the properties of polypropylene composites with seaweed fillers

Aicha DEHANE\*<sup>1</sup>, Dalila HAMMICHE<sup>1</sup>, Amar BOUKERROU<sup>1</sup>, Balbir Singh KAITH<sup>2</sup>

<sup>1</sup>Laboratoire des Matériaux Polymères Avancés, Département Génie des Procédés, Faculté de Technologie, Université de Bejaia, Algérie.

<sup>2</sup>Department of Chemistry, Dr. B.R. Ambedkar National Institute of Technology, Jalandhar, Punjab-144011, India

\*Corresponding author email\* [aicha.dehane@univ-bejaia.dz](mailto:aicha.dehane@univ-bejaia.dz)

Received 2 May, 2023 ; Accepted : 27 July 2023; Published: 29 July 2023

---

### Abstract

*The main focus of this work is to study the processability and characteristics of highly algae-loaded thermoplastic polymer composites. The seaweed powder was characterized in terms of morphology. Polymer/Alg composites were prepared by extrusion compounding. Polypropylene (PP) was used as the polymer matrix. During extrusion mixing, the composites were injection molded and characterized for their structural, morphological, and mechanical properties to determine the effect of the dispersant agent. The results for this research work has shown that algae can be used as a filler in the preparation of composites and that it is possible to play on the rate of the charge and of the dispersing agent to improve certain targeted properties for any specific application*

**Keywords:** seaweed powder; Polymer-matrix composites; Polypropylene Mechanical properties; chemical treatment.

---

## **I. Introduction**

Composite materials are those materials which built from two or more constituent materials with considerably different physical or chemical properties that when joined, to develop composite. Composite materials depend on the properties of constituent materials, the fibers and the resin used [1]. At present days, the advance composite material has been broadly used composite in the engineering field due to their noble mechanical properties. Advantages of this like as corrosion resistance, electrical insulation, more stiffness and strength, fatigue resistance, lesser in weight than metal, easy process ability at less energy requirement in tooling and assembly costs widely acceptable in structure applications [2].

Lots of advanced research literature is mentioned on composites reinforced with natural fibers so as to refine the mechanical resistance and mark them appropriate in many engineering applications [3].

Natural fibers are cheap, eco-friendly, lightweight, as well as competitive with synthetic material regarding material properties. To increase the performance of the bio-based fiber composite the raw material such as fiber and matrix material are chemically or physically modified [4].

Indeed, proper interfaces assure the transfer of load from the matrix to the stiff fibers. Wherefore, weak interaction notably drops the mechanical properties of the composite materials [5,6]. The compatibility and wettability between natural fibers and polymers can be improved by adding coupling and dispersing agents [7]. The treatment not merely enhances interfacial adhesion, but also provides better fibers dispersion [8]. Chemical treatments have been postulated as methods to improve the performance of biocomposite materials by enhancing the interaction of NFs with the polymeric matrix. The interaction is improved when undesirable organic components are removed and the functionality of cellulosic components on the fiber is modified [9,10]. Sobczak et al. reviewed the physical and chemical treatments to improve the interaction between natural fibers and the polymer matrix interface. These strategies lead to an increase in the capability for stress transfer at the interface [11]. Dispersants and coupling agents supply several advantages and are chosen based upon the application requirement. Dispersants adhere to the fiber surface but without a strong link with the matrix. Coupling agents also adhere to the fiber as well to the polymer through chemical bonds or through chain entanglement. Thus, the dispersant role

is to foster the homogeneity and limit defect sites by means of the agglomerate to give better dispersion of the fibers. Dispersants are a surface-active agent, being composed of two segments chemically different [12]. For this purpose, a dispersing agent It was applied in the current work BYK-W 980. It was a composite made of PP and seaweed powder. Study of mechanical and morphological properties of the compounds obtained in order to see the effectiveness of the dispersant on the PP/Alg compounds.

## **II. Experimental**

### **II.1. Material**

Commercial grade of polypropylene ISPLEN PP 040 C1E, supplied by REPSOL, with a melt index of 3.0 g/10 min (at 230 °C), were used as the matrix. Pickled seaweed was collected from the rocks of AINBINIANE ALGIERS.

The algae were initially washed with distilled water to remove dust and other waste then dried at room temperature for about a week. Then, they were dried in an oven at 40°C for about 48 hours and stored in closed containers. In order to obtain the seaweed flour, they are finely fractionated in a grinder (RestschZM200) with an ultra-centrifugal rotor at high speed, and then sassed using a 0.02 µm sieve. Methanol was 99% pure purchased from Changshu Yangyuan Chemical Company (Jiansu, China). The dispersing agent has been kindly given by **BYK-CHEMIE** whose properties are Trade Name: **BYK-W 980**.

Chemical nature Composition: Solution of a salt of unsaturated polyamine amides and acidic polyesters.

Acid value (mg KOH/g) = 129.

### **II.2. Seaweed fiber treatment**

Due to the hydrophilic character of natural fibers, they are considered incompatible with the hydrophobic polymer matrix and for this reason we have resorted to chemical treatment. In fact, the esparto fiber has been treated with a dispersing agent: BYK W-980. This chemical modification was carried out according to the following Protocol: 30g of esparto fiber was immersed in 100ml of methanol in a beaker with (2 pigs) by weight of dispersing agent, under stirring with a mechanical stirrer for one hour at room temperature. At the end of the reaction, the mixture was filtered and washed three times with acetone to remove excess reagent.

### **II.3. Preparation of composites**

The composite preparation process is as follows: the required quantities of raw materials such as PP, filler (processed and unprocessed) were loaded into the extruder. The mixture was

mixed using a twin screw extruder with a rotor speed of 80 rpm ; and the temperature of the extrusion operation was maintained in the range of 190 to 230°C. The extruded product was then cut into pellets and dried at room temperature. Then, the pellets were passed through an injection molding machine (Japan Steel Works, India) set at 190–210°C, 100 rpm and a holding pressure of 300 bar. Pellets were molded into conventional shapes and cooled to room temperature for testing and characterization. A reference sample of PP was also prepared in a similar manner.

## II.4. Characterization

### II.4.1. Fourier-transform infrared spectroscopy (FTIR)

The samples were dried at 80 °C for one hour and used for infrared spectroscopy analysis. Infrared measurements were made on an FTIR spectrophotometer (SHIMADZU FTIR-8400S). A resolution of 4 cm<sup>-1</sup> was used in the 4000-400 cm<sup>-1</sup> wavenumber region.

### II.4.2. Optical microscopy

The PP et PP/alg composites were imaged by Lecia DCM8 optical microscopy full version of 3D surface metrology. The samples were placed at the level of fracture and the results were obtained in the form of images.

### II.4.3. Mechanical properties

Tensile properties were obtained at room temperature according to ASTM D638 and using the universal test machine Instron 5969 equipped with an SVE 2 Non-Contacting Video Extensometer. The cross-head speed was fixed at 5 mm/min using a 50 kN load cell. For each material, six different specimens were subjected to tensile tests and average values of tensile strength, Young's modulus and elongation at break were calculated.

## III. Results and discussion

### III.1. Fourier Transform Infrared Spectroscopy (FTIR)

Fig.1 shows the FT-IR (a) spectra of the neat Alg and Alg/BYK W-980 ; The main changes in the spectrum of untreated algae compared to that of BYK W-980 treated algae are as follows :

A reduction in the intensity of the band at 3408 cm<sup>-1</sup> corresponding to the OH groups is observed, this reduction is due to the reduction of the hydrophilic character of the charge.

A band of average intensity towards 2927 cm<sup>-1</sup> translates the vibrations of elongations of the bonds C-

H of the group -CH and CH<sub>2</sub>.

Appearance of an absorption band at 1743 cm<sup>-1</sup>, this band corresponds to the elongation vibration of the C=O bond of the ester function existing in the charge. Decrease of the bands at 1627 cm<sup>-1</sup> corresponding to the deformation (H-O-H) of the water absorbed by the charge following the chemical treatments.

The broad bands in the region of 500-700 cm<sup>-1</sup> are due to residual water in the algae.

In parallel the spectrum of PP clearly illustrates the symmetric and asymmetric elongation vibrations of the C-H bonds of the aliphatic -CH<sub>2</sub> group and the CH<sub>3</sub> groups in the range between 2975 and 2840 cm<sup>-1</sup> and the symmetric deformation vibration of the -CH<sub>2</sub> group around 1464 cm<sup>-1</sup> (fig 1 (b)). The band around 1370 cm<sup>-1</sup> is characteristic of the symmetric deformation of the CH<sub>3</sub> groups at the end of the chains. An intense band is visualized around 820 cm<sup>-1</sup> and is characteristic of the balancing of the methylene groups - (CH<sub>2</sub>-) - when nis greater than 4 (-CH<sub>2</sub>-polymeric) [13].

Also, we notice that the FTIR spectrum of PP/Alg and PP/Alg/BYK W-980 is identical to that of PP but it reveals, in addition to the absorptions of PP, a characteristic band of the carbonyl group of the alga in the range [1580,1740] cm<sup>-1</sup> This is synonymous with the grafting of the filler onto the PP chains. With an increase in intensity of the bands at 1627 cm<sup>-1</sup> and 500-700 cm<sup>-1</sup> of PP/Alg/PYK W-980 by a for PP/Alg This is explained by the effect of chemical treatment by the dispersing agent and the filler/dispersing agent complex is well bound to the matrix [14].

It is noticed that the band around 2927 cm<sup>-1</sup> of the filler is dispersing and this reflects the elongation vibrations of the C-H bonds of the -CH and CH<sub>2</sub> group, which is synonymous with the grafting of the filler onto the PP chains.

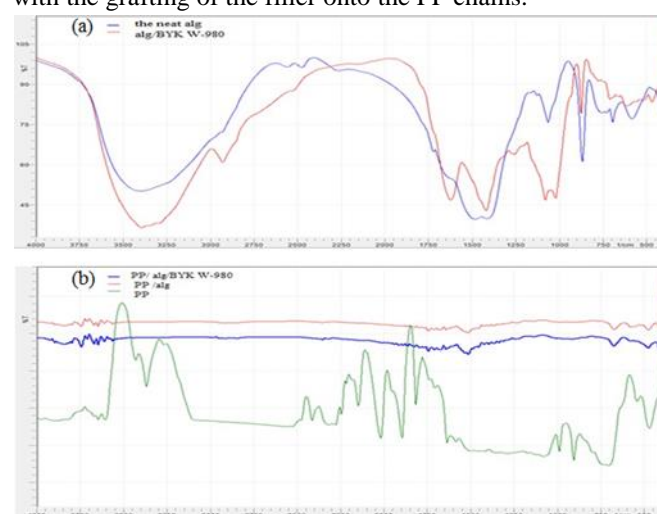
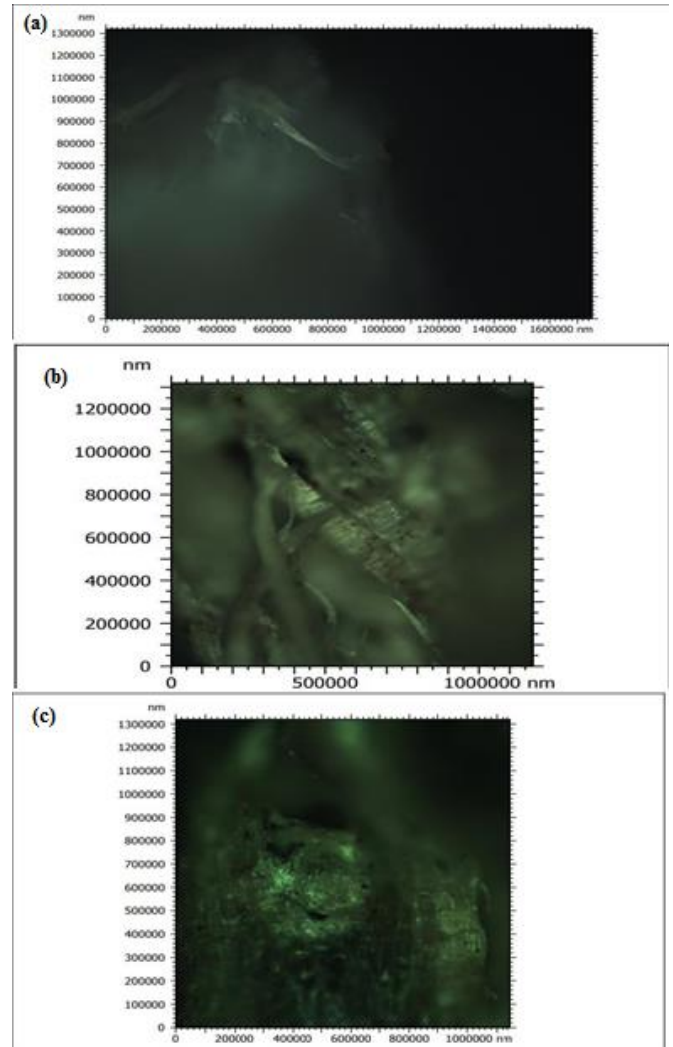


Figure 1. FTIR spectra : a) the neat Alg and alg/BYK ; b) the PP, PP /Alg and PP/ Alg/BYK W-980

### III.2. Optical microscopy

To investigate the phase morphology of PP/Alg (b), PP/Alg /BYK W-980 (c) and virgin PP (a), fracture surfaces at room temperature of the samples were observed by optical microscope after being gold coated (Fig. 2). It is clear that there are surface morphology distinctions between the different samples, as shown in (Fig.2). A visual aspect we observe the change of color in the case of the composite by to for to virgin pp due to add load. Seaweed occurs as flat, brittle flakes. The particle size distribution before and after sorting and mixing with PP will be discussed in the breaking section of sorted PP/Alg composites and unsorted PP/Alg composites sorted by to for the breaking section of virgin PP. for all samples have an irregular surface (Fig.2). In the case of composites filled with raw algae, it is noticed that the fibers detach and are taken from the PP matrix. As shown in photo (b) of Figure 2, the surfaces of the fibers are smooth and clean, which shows the weak interfacial adhesion between the fibers and the matrix with the presence of the aggregates of different sizes form on the surface of the PP. The photos show the presence of several knots. However, no clear gap is observed in the interfacial region between the PP matrix and the algal fiber for the PP/Alg/BYK W-980 systems photo (c) of Fig 2. Algae treated with BYK w-980 (Fig.2) are coated with layers of matrix material which significantly reduce the differences between them. This is probably due to the wetting of the algae by the dispersing agent which reduced the contrast between the fibers and the PP. These results are in agreement with previous studies which confirmed that the treatment with the dispersing agent BYK w- 980 of the natural fibers used as reinforcements, improves the cohesion between the fibers and the matrix of the corresponding composite materials [15]. That change in morphology is an indication of improvement in PP/Alg miscibility of the mixture after addition of the dispersing agent incorporation of algae.



**Figure 2.** Optical microscope micrographs of the fracture surface of a PP (a), (b) PP/Alg, PP/Alg /BYK-980.

### III.3. Mechanical properties

To reveal the effect of loads and treatment on mechanical properties such as tensile strength, elongation at break of PP/Alg mixture, tensile tests were carried out and the results are shown in ( Fig 3). Tensile strength (TS) and elongation at break (EAB) of the composites based on PP loaded with treated and untreated seaweed and virgin PP. According to number tensile results the strength of the composite reflects a considerable loss when adding seaweed fiber in PP matrix. Indeed, we are registering a drop compared to virgin PP. This is explained by poor dispersion of the algae fiber in the polymer which caused a weakening of the interfacial adhesion of the constituents of the composite increasing; therefore the transfer of constraints is not guaranteed. When BYK W-980 dispersant was added to (PP/Alg) composites, the Tensile strength (TS) and elongation at breaking (EAB) have been significantly improved. This significant improvement in tensile strength is generally attributed to better interfacial interaction and adhesion between the fibers and the polymer, leading to a better transfer of the stresses of

the fiber matrix, the incorporation of the loading with treatment implied a positive effect on the tensile strength and the elongation at break. Similar results have also been demonstrated by other authors for other polymers reinforced with natural fillers [16]. This increase indicates that the composite stiffness is increased. The stiffness and good dispersion of the fibers after processing result in interaction changes and chain mobility. Thus, the use of dispersing agent improves the dispersion state of the rigid fiber which prevents the movement of the continuous PP and increases the tensile strength which is decreased elasticity consequently the elongation at break increases. Finally, these results showed that the mechanical properties are in agreement with the morphological and structural results.

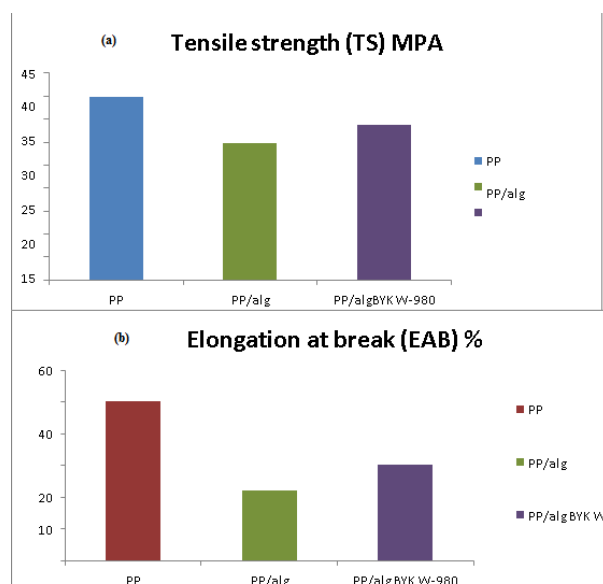


**Figure 3.** Tensile strength (TS) (a) and elongation at break (EAB) (b) of the composites based on PP loaded with treated and untreated seaweed and virgin PP.

#### IV. Conclusions

A PP matrix, untreated and W-980 dispersing agent treated algal fibers were used to develop composites. Mechanical, optical and structural properties were studied and compared.

Infrared results showed that the structure of the algae changed after the treatment process. This change was shown by the decrease of the peak at  $3408\text{ cm}^{-1}$  after the treatment corresponding to the -OH group.

Optical microscopy shows that the treatment improved the dispersion of the alga in the PP matrix, as well as the interfacial adhesion.

The mechanical properties were studied by the tensile test. This study reveals that the incorporation of seaweed powder into the PP matrix increases the

stiffness of the composites as well as the stress and elongation at break increase after the treatment compared to pure PP and PP/alg.

#### References

- [1] B.C. Mitra. Environment friendly composite material: Biocomposite and Green Composite. *Defense Sci J*, 64, 244-261, 2014.
- [2] V.K. Thakur, A.S. Singha, and M.K Thakur. *Green Composites from Natural Cellulosic Fibers*, Germany: GmbH & Co. KG, 2011.
- [3] P.K. Bajpai, S. Inder deep and M. Jitendra. Comparative studies of mechanical and morphological properties of polylactic acid and polypropylene based natural fiber composites. *J Reinforced Plast Compos*, 31, 1712-1724, 2012.
- [4] A. Sayeed. Mechanical properties and damage analysis of jute/polypropylene hybrid nonwoven geotextiles. *Geotextiles and Geomembranes*, 37, 54–60, 2013.
- [5] G. Koroni, A. Silva, M. Fontul. a review of adequate materials for automotive applications. *Compos. Part B Eng.* 44, (1) , 120-127, 2013.
- [6] P. Wambua, J. Ivens, I. Verpoest. Natural Fibres Can They Replace Glass in Fibre Reinforced Plastics. *Compos. Sci. Technol.* 63, 1259-1264, 2003.
- [7] Y. Xie, A. Hill, Z. Xiao, H. Militz, C. Mai. Silane coupling agents used for natural fiber/polymer composites: A review *Compos. A: Appl. Sc. Manuf.* 4,1, 806-819, 2010.
- [8] A. C. Gowman, M. C. Picard, L.T. Lim, M. Misra, A. K. Mohanty Fruit waste valorization for biodegradable biocomposite applications: A review. *BioRes.* 14(4), 10047-10092, 2019.

*e-ISSN : 2800-1729*

- [9] L. Sobczak, O. Brüggemann, R.F. Putz, Polyolefin composites with natural fibers and woodmodification of the fiber/filler–matrix interaction, *J. Appl. Polym. Sci.* 127, 1–17, 2013.
- [10] X. Li, L. Tabil, S. Panigrahi, Chemical treatments of natural fiber for use in natural fiber- reinforced composites: a review, *J. Polym. Environ.* 15, 25–33, 2007.
- [11] X. Li, L. Tabil, S. Panigrahi. Chemical treatments of natural fiber for use in natural fiber-reinforced composites: a review, *J. Polym. Environ.* 15, 25–33, 2007.
- [12] C. DeArmitt, R. Rethon, in Meyer Kutz (eds), *Applied Plastics Engineering Handbook Processing and Materials Plastics Design Library*, 441-454, 2011.
- [13] W.H. Ferreira, R. Rachel, R. Khalili, J.M. Mario, Figueira Junior, C.T. Andrale. Effect of organoclay on blends of individually plasticized thermoplastic starch and polypropylene. *Industrial Crops and Products* 52,38– 45, 2014.
- [14] Y. Dong, J. Marshall, H. J. Haroosh, S. M. Z. Adam, D. Liu, X. Qi, K. T. Lau, Tea consumption and the risk of depression: a meta-analysis of observational studies. *Compos. Part A Appl. Sci. Manuf.* 76, 28, 2015.
- [15] H. Ibrahim, D. Hammiche, A. Boukerrou, C. Delaite, Effect of Dispersant Agent Content on the Properties of Composites Based on Poly (Lactic Acid) and Alfa Fiber. *Mater. Today Proc.* 2020, <https://doi.org/10.1016/j.matpr.2020.05.120>.
- [16] V. Fiore, L. Botta, R. Scaffaro, A. Valenza, A. Pirrotta. PLA based biocomposites reinforced with Arundo donax fillers. *Compos Sci Technol.* 105:110e7, 2014.